

THE HOMEBOX PROTEIN HOXC10 IS OVEREXPRESSED IN BREAST CANCER
AND INCREASES RESISTANCE TO CHEMOTHERAPY

by
Helen Sadik

A dissertation submitted to Johns Hopkins University in conformity with the requirements
for the degree of Doctor of Philosophy

Baltimore, Maryland

August, 2013

© 2013 Helen Sadik

All Rights Reserved

ABSTRACT

Background. Drug resistance is a major limiting factor in the success of targeted cancer therapies resulting in failure of treatment. A molecular understanding of the underlying mechanisms is essential to predict, prevent and overcome drug resistance. Though many pathways have been studied, key factors driving these pathways have not been largely identified.

Methods. Using a tiling array of all four HOX clusters, we identified HOXC10 as being among the highly overexpressed genes in breast cancer. Then using a panel of cell lines that either stably overexpress exogenous HOXC10 or cell lines with stably downregulated endogenous HOXC10 (mediated by shRNA), we investigated the role of HOXC10 in proliferation, response to chemotherapy treatment and repair of DNA damage. Mechanistically, we studied the consequence of HOXC10 binding to CDK7 during response to chemotherapy. Finally, we investigated the importance of HOXC10 as a prognostic marker in breast cancer.

Results. HOXC10 is frequently overexpressed both in primary breast tumors and distant metastatic tissues. HOXC10 promotes continuous growth by facilitating G1/S progression and replication resumption with higher E2F1 activity. Higher levels of HOXC10 expression is also associated with worse relapse-free survival, and overall survival in chemotherapy treated patients. In fact, HOXC10 is upregulated in chemoresistant MCF7 cell lines, and MDA-MB-231 and SUM-159 xenografts. When cells are exposed to DNA damaging agents, HOXC10 suppresses apoptosis, enhances DNA damage repair and NF- κ B activity, reducing susceptibility to drug treatment. Further investigation to HOXC10 binding partners after chemotherapy treatment led to the finding that HOXC10 binds to and stimulates the kinase activity of CDK7 towards its

substrate, RNA polymerase II, and the association of CDK7 with XPD. This allows HOXC10 to support the resumption of transcription and the recovery of cells after DNA damage. Consequently, inhibiting CDK7 pharmacologically or reducing its levels using siRNA reduced the protective effect of HOXC10 on drug-treated cells.

Conclusions. These data suggest that HOXC10 plays a key role during progression and recurrence of breast cancers through modulating different survival pathways. Therefore, decreasing the levels or function of HOXC10 in breast cancers might be a promising strategy to reduce chemotherapy resistance.

Readers/Advisors: Dr Saraswati Sukumar; Dr Fred Bunz

ACKNOWLEDGMENTS

First of all, I want to thank all my family members and friends for their continuous support during the completion of my thesis work, and for understanding my crazy schedule, especially in the weekends. I wouldn't be here today without your unconditional love during all the stages of my life. Special thanks to Dr Joseph Akar for nurturing my ambition, Georges Issa for changing me to the best, Dimiter Avtanski and Joyce Helou for teaching me how to be crazy and of course, to Firas Barakat for returning the hope and smile to my life. I will specifically dedicate this work to my mother.

Second, I want to thank all Breast Cancer Program and CMM staff, professors and students, in particular, Leslie Lichter and Colleen Graham. I will never forget the first day I met you and how you hugged me and welcomed me to USA.

Third, I could spend pages writing about and thanking current and past Sukumar lab members. They were not just my colleagues, but truly my second family. We shared laughs, dreams, sadness and importantly, sushi! When I was in doubt about myself and my work, they were always here to push me forward. My work might get forgotten in a month, a year or a decade, but I hope they will always remember me as the "crazy workaholic", the "I am always right" or the "superwoman".

Finally, I can't express enough my gratitude and thanks to Dr. Saraswati Sukumar, my mentor, colleague, and second mother, who allowed me to grow both at the professional and the personal levels. When I walked to her office the first day, I would have never imagined I will walk out after 6 years as this mature, accomplished professional. Under her upright supervision and tough guidance, I carry today the strongest tools to pursue and achieve the dream I left everything for: Finding a cure for cancer... Let the real journey begins!

TABLE OF CONTENTS

Title	i
Abstract	ii
Acknowledgement	iv
Table of Contents	v
List of Tables	vii
List of Figures	viii
Chapter 1: Introduction	1
1.1 Breast cancer prevalence, treatment and chemoresistance	1
1.2 Role of HOX genes: Beyond normal development to key involvement in oncogenesis	5
Chapter 2: Materials and Methods	9
Chapter 3: HOXC10 is preferentially and functionally overexpressed in breast tumors	18
3.1 HOXC10 is frequently overexpressed in breast cancer	18
3.2 HOXC10 overexpression increases aggressiveness of cancer cells	21
Chapter 4: HOXC10 promotes proliferation by facilitating G1/S transition during cell cycle progression	23
4.1 HOXC10 increases proliferation of cancer cells	23
4.2 HOXC10 facilitates G1/S transition	26

4.3	HOXC10 indirectly activates E2F1 pathway to promote proliferation	31
Chapter 5:	HOXC10 actively promotes chemotherapy resistance and its expression after treatment has poor prognosis value	37
5.1	High levels of HOXC10 expression correlates with poor prognosis in treated patients	37
5.2	HOXC10 is induced during chemotherapy resistance	39
5.3	HOXC10 overexpression decreases susceptibility to chemotherapy	44
5.4	HOXC10 stimulates DNA damage repair and checkpoint recovery to promote long-term survival	53
Chapter 6:	HOXC10-CDK7 interaction: a new model and target for chemoresistance	60
6.1	HOXC10 binds to CDK7 in vivo after chemotherapy treatment	60
6.2	Inhibiting CDK7 reverses chemoresistance developed by HOXC10 overexpression	66
Chapter 7:	Discussion	72
Chapter 8:	References	79
Curriculum Vita		87

LIST OF TABLES

Table 1 Cell cycle distribution

27

LIST OF FIGURES

Figure 1.1	Stages of breast cancer progression	2
Figure 1.2	Mammalian Hox clusters arrangement and expression	7
Figure 3.1	Genomic analysis reveals that HOXC10 is commonly overexpressed in breast cancer	19
Figure 3.2	Real-time PCR in tumors and cell lines validated HOXC10 overexpression	20
Figure 3.3	High-levels of HOXC10 leads to more aggressive in-vitro and in-vivo phenotypes	22
Figure 4.1	HOXC10 promotes the proliferation of cells under optimal and non- optimal conditions	24
Figure 4.2	HOXC10 DNA binding ability is required for promoting proliferation	25
Figure 4.3	Knock-down of HOXC10 arrested cells at late G1	28
Figure 4.4	Cells failed to start new origins efficiently	29
Figure 4.5	Cells exhibit a delayed G1/S transition	30
Figure 4.6	HOXC10 activates E2F1 activity	33
Figure 4.7	HOXC10 transcriptional ability is required for E2F1 activation	34
Figure 4.8	The proliferation signature is higher in the presence of HOXC10	35

Figure 4.9 Higher protein level or activity of cell cycle proteins validated the RT-PCR data	36
Figure 5.1 HOXC10 expression has negative prognostic value	38
Figure 5.2 HOXC10 is functionally induced in an in-vitro resistance system	41
Figure 5.3 HOXC10 expression is induced in an in-vivo resistance system	42
Figure 5.4 HOXC10 expression is induced after short-term treatment	43
Figure 5.5 Loss of HOXC10 increases long-term drug susceptibility	46
Figure 5.6 HOXC10 modulates short-term drug susceptibility	47
Figure 5.7 HOXC10 decreases apoptosis	48
Figure 5.8 HOXC10 decreases apoptosis as measured by western blot	49
Figure 5.9 HOXC10 decreases apoptosis as measured by qRT-PCR	50
Figure 5.10 HOXC10 protects cells from doxorubicin in-vivo	51
Figure 5.11 HOXC10 increases baseline and induced NF- κ B activity	51
Figure 5.12 No difference in doxorubicin accumulation or retention is observed	52
Figure 5.13 HOXC10 activates DNA repair in response to DNA crosslinks	55
Figure 5.14 HOXC10 effectively protects cells from UV exposure	55
Figure 5.15 Comet assay shows a better DNA repair with HOXC10	56
Figure 5.16 More residual DNA damage is observed in the absence of HOXC10	

as measured by γ H2Ax foci	57
Figure 5.17 No difference in the kinetics of DNA damage induction is observed	57
Figure 5.18 HOXC10 doesn't modulate initial DNA damage response	58
Figure 5.19 HOXC10 is required for efficient checkpoint recovery	59
Figure 6.1 HOXC10 binds to CDK7 during DNA damage response	62
Figure 6.2 HOXC10-CDK7 interaction is independent of their DNA binding ability	62
Figure 6.3 CDK7 binds TFIIH more efficiently in the presence of HOXC10	63
Figure 6.4 CDK7 activity towards RNA Pol II is reduced upon HOXC10 kd	64
Figure 6.5 CDK7-XPD association is increased upon HOXC10 expression	65
Figure 6.6 CDK7 KD restored response to chemotherapy in SUM159	68
Figure 6.7 CDK7 KD restored response to chemotherapy in MCF10A-Ras	69
Figure 6.8 CDK7 inhibition by drugs restored response to chemotherapy	70
Figure 6.9 CDK7-specific inhibition reduced acquired chemoresistance	71
Figure 7 Model of HOXC10 function	78

CHAPTER 1

Introduction

1.1 Breast cancer prevalence, treatment and chemoresistance

According to the National Cancer Institute, 1 in 8 U.S. women will develop invasive breast cancer during the course of her lifetime, and breast cancer is the most commonly diagnosed cancer among women (30% of all cancers). Besides lung cancer, breast cancer death rates are higher than those for any other cancer (1).

Breast cancer usually develops in the cells of the ducts (the milk passages from the glands to the nipple) or of the lobules (the milk-producing glands), and less commonly in the stromal tissues. Like many cancers, breast cancer progresses through identifiable stages of development from hyperplasia to atypical hyperplasia (the precancerous stages) to carcinoma in situ and finally to invasive carcinoma when the cancer cells break through the basement membrane and spread to the lymph nodes or to other organs (Figure 1.1). Only 5% of breast cancers are familial in origin, with BRCA1 or BRCA2 mutations being the most common inherited susceptibility genes; however, the majority develops through spontaneous, non-inherited genetic and epigenetic modifications.

With the advance of microarray-based gene expression profiling, it became obvious that breast cancer encompasses a heterogeneous group of diseases with distinct molecular features. At least 4 different subtypes were identified: Luminal A (Estrogen receptor (ER) and/or progesterone receptor (PR)-positive; human epidermal growth factor receptor 2 (HER2)-negative), Luminal B (ER and/or PR-positive; HER2-negative or HER2 over-expressed/amplified), HER2-enriched (HER2 over-expressed or amplified; ER and PR

negative) and Basal-like (triple-negative: ER, PR and HER2 negative) (2). These molecular subtypes exhibit differences in prognosis and treatment sensitivity, with the Luminal A having the best outcome and the basal-like having the worst prognosis.

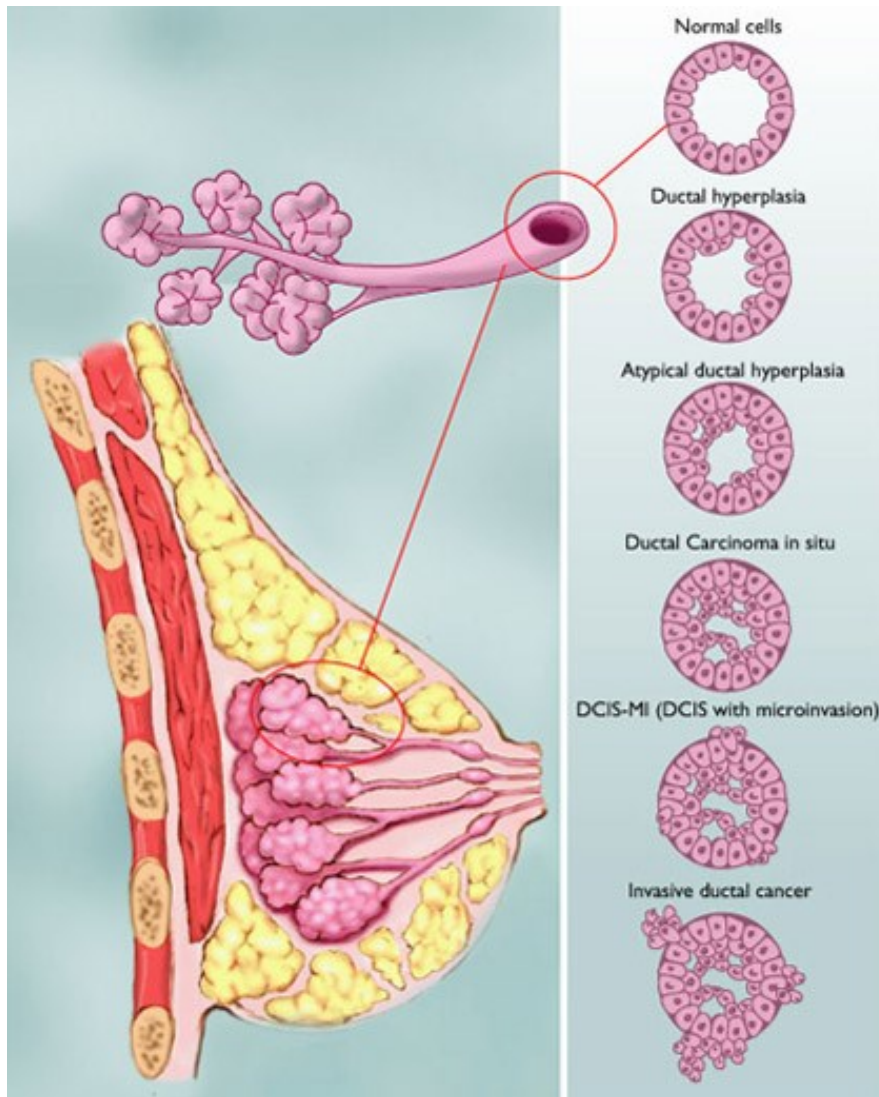


Figure 1.1. Stages of breast cancer progression. Adopted from

<http://www.breastcancer.org/symptoms/types/dcis/diagnosis.jsp>

Accessed date: 08/14/2013

Although the death rates have been decreasing due to the advances in treatment, the earlier detection through screening and the increase of awareness, the decline is still not significant due to the high resistance and recurrence rate. This drove efforts to develop prognostic and predictive biomarkers within each subtype that can effectively guide targeted therapies as well as distinguish patients who are undertreated from those who are overtreated. Some of the single emerging biomarkers are Ki67, Cyclin D1 and Cyclin E, TOP2A, uPA, circulating and disseminated tumor cells and tumor-derived cell-free circulating DNA and microRNA (3). Currently, multigene assays are commercially available to guide some treatment options, and are regarded as more objective, reproducible and precise compared to the histopathology assessment. Some of these tests are: Oncotype Dx, Adjuvant! Online, MammaPrint, PAM50 and molecular grade index (Theros MGI). However, these assays are expensive, and their clinical utility is still not clear. More decision impact studies are definitely needed.

Different treatment options exist for patients with breast cancer, the choice of which depends on both histological and molecular characteristics of the tumor (tumour size, nodal status, histological grade, and cancer subtype (ER, PR and HER2 status)). The standard therapies are surgery, radiation, and chemotherapy, hormonal or targeted therapies. New types of treatment options are currently undergoing clinical trial testing, including immunotherapies, nanotherapy, gene therapy and stem cells transplantation. The current chemotherapy drugs used include: anthracyclins (i.e. doxorubicin), taxanes (anti-microtubules, i.e. paclitaxel and docetaxel), antimetabolites (i.e. 5FU, gemcitabine), alkylating agents and platinum compounds (i.e. cyclophosphamide, cisplatin, carboplatin) (4).

It is estimated that drug resistance contributes to treatment failure in most patients with metastasis (5). This resistance may be intrinsic or acquired during the course of

treatment, the latter leading sometimes to cross-resistance, even to structurally and mechanistically unrelated chemotherapeutics. In breast cancer, chemotherapies are initially active in 90% of primary breast cancers and 50% of metastases. However despite initial tumor response, approximately 30% of treated patients develop a systemic recurrence (4). This elevated rate of recurrence most probably reflects the presence of micrometastatic disease in 10% to 30% of lymph node-negative and in 35% to 90% of lymph node-positive patients at the time of diagnosis. For these cancer cells to continuously overcome the toxic effects of chemotherapeutic drugs, they have to develop a multidimensional response, which include alterations in the drug target; decrease in drug accumulation; drug inactivation; processing of the drug-induced damage; and evasion of apoptosis (6). There is therefore a need to develop therapies to block these mechanisms as well as to develop better prognostic and predictive markers for drug response.

The common use of the immunohistochemically determined proliferation marker Ki67 to assess the aggressiveness of breast cancers has emphasized the importance of proliferation in prognosticating tumor behavior. With the current ability to assess the expression of thousands of gene loci in tumors by microarray analysis, expression patterns of groups of genes have emerged that help predict tumor behavior. In particular, the proliferation signature (7) has been linked to poor outcome in breast cancer patients (8-11). Although the identity of genes in this signature between tumors or studies is variable, they invariably include genes involved in the fundamental processes of cell cycle and proliferation, such as STK6, PLK1, AURKA, E2F1, TOP2A, FOXM1, MKI67 and the MCM genes (12). Specifically, high E2F1 expression and its signature have been associated with tumors of high-grade, resistance to chemotherapy and poor patient survival in different cancers (13-16). Although E2F1 induces apoptosis

in response to DNA damage, it can also promote drug resistance through triggering the autoregulatory circuit of E2F1-p73/DNp73-miR-205 (17, 18).

Many chemotherapy treatments induce DNA damage, which trigger cancer cells to activate their repair machinery. When the damage is extensive and remains unrepaired, cells undergo apoptosis (19). There are several pathways involved in DNA repair. Nucleotide excision repair (NER) is one of the major mechanisms involved in the repair of DNA adducts, specifically inter- or intra-strand cross links and pyrimidine dimers, the kind of damage that results in cells from the use of alkylating or platinum-derived agents. One of the rate limiting factors in NER is ERCC1, and its expression is linked to poor response to platinum-based chemotherapy in ovarian, gastric, non-small cell lung cancers and colorectal cancers (20-24). The NER pathway is a complex process involving at least 17 different proteins, and 2 sub-pathways: global genome repair (GGR) and the transcription-coupled repair (TCR) pathway. Interestingly, many components of the TFIIH complex- which is involved in transcription- are also important in promoting the NER pathway, through mediating the sensing of damaged DNA, the recruitment of NER components and the preparation of DNA for repair (25).

1.2 Role of HOX genes: Beyond normal development to key involvement in oncogenesis

The HOX genes belongs to the evolutionarily conserved homeobox superfamily, characterized by the 61-amino acid DNA binding domain (homeodomain). First identified in *Drosophila melanogaster* as the genes responsible for their correct spatial body development, homologs of these genes were soon after found throughout the kingdom *Animalia*, with varying roles and numbers within each species and its anatomic complexity. In humans, there are 39 HOX genes organized into four paralogous clusters,

HOX-A to -D (26). Well known as transcription factors, they can function either as monomer or as heterodimers with members of the three amino-acid-loop extension (TALE) cofactors.

During embryonic development and maintenance of adult homeostasis, their expression follows a strict spatio-temporal pattern, which reflects their order in the cluster, according to 3 principles (Figure 1.2):

- 1) Spatial colinearity: A HOX gene position from 3' to 5' within the cluster corresponds to its expression within the animal along the A-P axis
- 2) Posterior prevalence: HOX genes that lie more 5' within the cluster will have a dominant phenotype to those more 3'
- 3) Temporal colinearity: A HOX gene position from 3' to 5' corresponds to its order of expression during the time of development.

However these principles are more complicated in mammals, given the presence of 4 HOX clusters that arose by duplication, and paralleling the high complexity of their organ systems. Not surprising then, is that there is functional redundancy among the HOX genes, especially among the paralogs.

Beyond development, aberrant expression of the HOX genes has been associated with a variety of diseases including cancers. Abate-Shen theorized 3 basic modes of HOX deregulation during oncogenesis: a) expression of HOX genes within a tissue in a pattern temporo-spatially different from normal, mature tissue; b) expression of HOX genes within a tissue that are normally never expressed within that tissue type (gene dominance); and c) downregulation or silencing of HOX genes in a tissue when they should be normally expressed (mainly epigenetic regulation).

Extensive recent research has demonstrated that the HOX genes can regulate many important processes such as differentiation, apoptosis, motility, receptor signaling,

wound healing and angiogenesis. In breast cancer, HOXB7 and HOXB13 are upregulated and drive tamoxifen resistance through distinct mechanisms (27, 28). On the other hand, loss of expression of HOXA5 and HOXA10 is observed in high-grade breast tumors and leads to decrease in apoptosis and p53 expression (29-31).

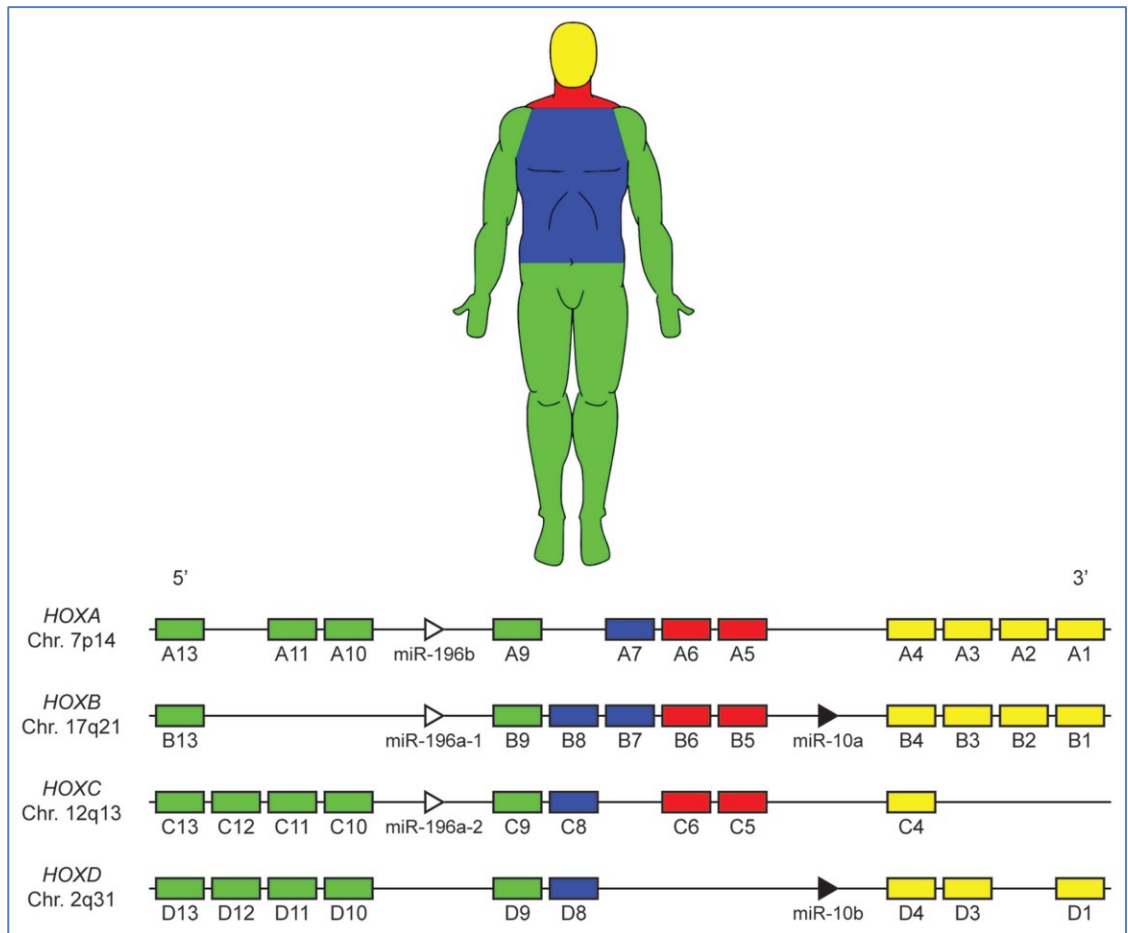


Fig 1.2. Mammalian Hox clusters arrangement and expression. Adopted from Ref (32).

Extensive recent research has demonstrated that the HOX genes can regulate many important processes such as differentiation, apoptosis, motility, receptor signaling, wound healing and angiogenesis. In breast cancer, HOXB7 and HOXB13 are upregulated and drive tamoxifen resistance through distinct mechanisms (27, 28). On the other hand, loss of expression of HOXA5 and HOXA10 is observed in high-grade breast tumors and leads to decrease in apoptosis and p53 expression (29-31).

HOXC10 is unique among the HOX genes in that it has 2 D-boxes required for efficient ubiquitylation and protein destruction by anaphase promoting complex (APC) (33). Therefore, HOXC10 protein- and not the mRNA- oscillates during the cell cycle and regulates mitotic progression and proliferation. HOXC10 has also been shown to bind to (34), and participate in the function of DNA replication origins in human cells (35) and is important in tissue regeneration (36). In cancer, high HOXC10 expression is observed in invasive cervical cancers (37) and in lymph node-positive breast carcinomas (38). Recently, HOXC10 was shown to be up regulated by estrogen, myeloid/lymphoid or mixed-lineage leukemia MLL3 and MLL4 in breast cancer cell lines (39).

We have previously reported that HOXC10 is one of the highly overexpressed genes in a panel of primary breast tumors and distant metastasis (40). Here, we demonstrate that in unstressed conditions, HOXC10 drives cell proliferation by facilitating transition from G1 to S phase and by enhancing E2F1 activity. However, upon DNA damage, HOXC10 protects cells from apoptosis by binding to CDK7 and enhancing DNA repair, mainly through the NER pathway. This eventually leads to decrease in susceptibility to chemotherapy. In line with this finding, chemotherapy-resistant cell lines and xenografts have higher expression of HOXC10. Lastly, high HOXC10 expression in breast cancer predicts a poorer outcome in patients undergoing chemotherapy.

CHAPTER 2

Materials and Methods

Cell Lines, Constructs, and Reagents. All cell lines were purchased from ATCC. MCF10A-Ras was established through stable transfection of LXS-N-K-Ras vector into MCF10A. MCF7 wt and resistant sublines were a kind gift of Dr Parissenti (41). Doxorubicin was purchased from Sigma, paclitaxel and gemcitabine from Tocris Bioscience and carboplatin, BS-181 and SNS-032 from Selleckchem. All other reagents were from Sigma. Human HOXC10 cDNA was purchased from Thermo Scientific and cloned into the EcoRI and ClaI sites of pLPCX for retroviral production. TRC lentiviral Human HOXC10 shRNA (set of 4 clones) were purchased from Thermo Scientific. FlexiTube siRNA for HOXC10 (SI04296621), E2F1 (SI00300083) or CDK7 (SI02664795) were purchased from Qiagen. For transient knockdown, cells were seeded at low density and transfected for 48h with the indicated siRNA using Lipofectamine reagent. Retrovirus and lentivirus were produced in HEK 293T cells, collected and used for cell infection with DEAE-dextran. Stable pools of overexpression or knockdown of HOXC10 in cell lines were selected by puromycin. For the generation of deletion constructs, full length myc-tagged HOXC10 was cloned in pCDNA3.1-Neo at EcoRI and XbaI sites. Four deletion constructs were created by PCR-directed mutagenesis: Δ N-term (AA 1-15), Δ Phosph (AA 182-229), Δ Homeodomain (AA 268-327) and Δ 3rd helix (AA 309-325).

Human Tissue Samples. Normal breast organoids, fresh frozen primary breast tumors and metastatic breast carcinoma tissues were obtained following approval from the Johns Hopkins Institutional Review Board (IRB) and processed as previously described (28). Samples were lysed with Trizol (Invitrogen) and total RNA was extracted.

Real-time Quantitative PCR (RT-qPCR) Analysis. Cells were seeded in 6 well plates and harvest at equal density or after treatment with TRIzol. 2ug of RNA was reversed transcribed using M-MLV (Promega). Primers were designed using the Universal Probe Library Software (42) to span an intron. qRT-PCR was then conducted using the Maxima SYBR Green/ROX Master Mix (Fermentas) per manufacturer protocol. Gene expression was analyzed by the $\Delta\Delta C_t$ method, with GAPDH expression used for normalization.

Soft Agar Colony Formation Assay and Matrigel Invasion Assay. For anchorage independent growth, six-well plates were first covered with a 0.6% agar layer. 3×10^3 cells were then cultured in complete media within a 0.3% agar layer. Medium was added as the top layer. The plates were incubated for 7 days, after which the colonies were counted and photographed.

The BD BioCoat Matrigel Invasion Chamber assay system was used to study the in-vitro invasion ability of cells according to the manufacturer's instructions. In brief, 10×10^3 cells in serum free medium were added to the insert and allowed to invade the matrigel migrating towards a FBS-rich medium. After 20h, noninvading cells were removed by scrubbing with a cotton-tipped swab. The membrane was collected, fixed and stained with 1.25% crystal violet. The number of invading cells was counted under a light microscope. Both these experiments were carried out in triplicate.

Tumor Xenograft Studies. 3- to 4-wk-old BALB/c nu/nu athymic mice (Sprague–Dawley; Harlan, Madison, WI) were used, and study approved by Johns Hopkins Institutional Animal Care and Use Committee (IACUC). A total of 3×10^6 cells were suspended in 100 μ L PBS/Matrigel (1:1) and injected subcutaneously into both flanks of each mouse. Xenografts were measured once per week. In experiments with drug treatment, when the average tumor size reached 100 mm³, doxorubicin was

injected intravenously at a dosage of 4 mg/kg body weight, once per week, for 3 consecutive weeks. At necropsy, primary tumors were collected and lysed with TRIzol for RNA extraction.

Growth Assay. Cells were seeded in triplicate in 12 well plates (2000 cells/well). At the indicated time, cells were fixed with formalin and stained with crystal violet. The plates were then photographed. For quantification, the dye was solubilized by 10% acetic acid, and absorbance was measured at 560nm.

Flow Cytometry Analysis. For propidium iodide staining, cells at 70-80% confluency or after double thymidine synchronization were collected and permeabilized overnight with cold 70% ethanol at -20°C . Cells were then pelleted and resuspended in an isotonic buffered PI-staining solution containing RNase A (0.1 mg/ml) and propidium iodide (20 $\mu\text{g}/\text{mL}$). Samples were run on the BD FACSCalibur system (Becton Dickinson), and data analyzed using WinMDI 2.9 software.

For BrdU incorporation assay, cells were incubated with 10 μM BrdU (Invitrogen) for 1h. Labeled cells were harvested and fixed in 70% ethanol. Cellular DNA was denatured using 2N HCl with 0.5% Triton X-100, neutralized with 0.1 M sodium tetraborate ($\text{Na}_2\text{B}_4\text{O}_7 \cdot 10\text{H}_2\text{O}$, pH 8.5), and BrdU was detected using the Alexa Fluor® 488 conjugated anti-BrdU (Millipore). After staining for 1h, cells were suspended in 1 ml of the PI-staining solution, and run on the BD FACSCalibur flow cytometer to determine BrdU incorporation and DNA content.

DNA Fiber Assay. Exponentially growing cells were labeled for sites of ongoing replication with IdU (50 μM) for 20 min, followed by exposure to HU (4mM). HU was removed by washing cells four times with PBS before labeling with media containing CldU (50 μM) to mark the sites of replication recovery. After trypsinization, cells were

washed with cold PBS, resuspended in lysis buffer (0.5%SDS, 50mM EDTA, and 200mM Tris·HCl), and spread on tilted glass slides, facilitating the spread of genomic DNA into single-molecule DNA fibers by gravity. Next, the slides were fixed in acetic acid and methanol (1:3 ratio). DNA was then denatured by treating fibers with 2.5MHCl, neutralized, washed first with 1× PBS (pH 8.0), and subsequently washed three times with 1× PBS (pH 7.4). This was followed by blocking with 10% bovine serum and 0.1%Triton-X in PBS (60 min) and incubation with primary antibodies against IdU (BD Biosciences) and CIdU (Novus Biologicals), followed by incubation with secondary antibodies for 1 h each. Fibers were analyzed using ImageJ software.

Luciferase Assay. 1×10^5 cells were seeded in 12-well cell culture plates, and transfected with a total of 1.6 μ g of plasmids including reporter, expression and pCMV- β -galactosidase plasmids using Lipofectamine 2000. After 48 h, cells were lysed and luciferase activity was measured using a microplate reader (BMG LABTECH). β -galactosidase activity was measured using the reporter assay system (Promega) according to the manufacturer's instructions, and used to normalize luciferase activity. The responsive reporter plasmids 2xE2F-dhfr (wt or mut), E2F-DNA polymerase α and NF- κ B-luc (I κ k2-IFN-luc wt or mut) were a kind gift of Dr. Miguel R. Campanero (43), Dr. William G. Kaelin, Jr. (44) and Dr. Joel L. Pomerantz (45) respectively. TOPFlash plasmid was purchased from Addgene (46).

Clonogenic Cell Survival Assay. Exponentially growing cells were treated with different chemotherapy drugs or with ultraviolet (41) light. After 24h, drug was washed out and cells were reseeded in triplicate at low density in 6 well plates (1000-2000 cells/well) to allow damage repair and the recovery and growth of resistant cells. After 1-2 weeks, viable colonies were fixed, stained with crystal violet and counted.

MTT assay. 2.5×10^3 cells/well were plated in 96-well plates in triplicate and treated with the indicated drug concentrations, alone or in combination. After 48h, MTT solution (5 $\mu\text{g/ml}$) was added, cells incubated for 3h, dissolved in DMSO and absorbance at 560 nm was measured, with background at 670 nm subtracted. Values are expressed as percent survival of the vehicle-treated control (given as 100%). In CDK7 knockdown experiments, cells were seeded at low density in 96 well plates, transfected with scramble or siCDK7. After 24h, cells were treated with drugs at the indicated concentrations.

Caspase 3/7 Activity. Caspase-3 and -7 activities were measured with the Caspase-Glo[®] assay kit (Promega) according to the manufacturer's instructions. Briefly, cells were seeded in 96 well plates and treated with doxorubicin (1 μM), gemcitabine (1 μM), taxol (0.5 μM), docetaxel (0.5 μM) or carboplatin (100 μM). After 24h, the drug was removed and fresh media containing Caspase-Glo reagent was added to each well. The plate was incubated at room temperature for 1 hour, and luminescence was measured in the microplate reader. Values are expressed as percent activity of the vehicle-treated control.

Western Blot Analysis. Cells were seeded in 6 well plates and treated with the appropriate drug. At the indicated time, they were lysed with RIPA buffer. 25 μg of extracted protein were vertically electrophoresed on 4-12% Bis-Tris NuPage Novex Gel in MOPS SDS running buffer (Invitrogen), then transferred to Hybond C Extra membrane (GE Healthcare). Membranes were stained with Ponceau stain to confirm protein transfer, then blocked with 5% powdered milk in PBS with 0.2% Tween-20 (PBST) for one hour. Membranes were probed with primary antibody in 5% milk/PBST at 4°C overnight, rinsed with PBST, then probed with secondary antibody (GE Healthcare) at 1:2000 dilution in 5% milk/PBST for 1h. After rinsing with PBST, membranes were

treated with ECL Plus Detection Reagent (GE Healthcare) for 1 minute, and exposed to Hyblot CL autoradiography film to determine protein expression. Antibodies to CDK7 and XPD were purchased from Santa Cruz; BCL-xL and BIRC3 from Abcam. All other antibodies were from Cell Signaling.

Cellular Retention of drugs. Doxorubicin (dox) is fluorescent which allows easy monitoring of its intracellular accumulation quantitatively by flow cytometry. Cells were treated with the 200 nM of dox for 4h to detect dox accumulation. It was then wash out, and cells were left for another 4h to measure dox retention in them. Cells were collected in PBS and the fluorescence intensity (FL2-H) was measured on FACSCalibur flow cytometer.

Host-Cell Reactivation Assay. To induce the formation of DNA adducts, pGL3-basic (Promega) was irradiated with different doses of UV light in Stratalinker® UV Crosslinker 1800 (Stratagene) or treated with 100 or 1000nM cisplatin. To form double strand breaks, the vector was digested with HindIII. 1 µg of the treated vector was transfected into cells along with pCMV-β-galactosidase. Luciferase and β -galactosidase activities were measured after 48h as above.

Comet Assay. The alkaline Comet assay was carried out using a CometAssay Kit (Trevigen) according to the manufacturer's protocol. Briefly, cells were treated with dox (200nM) or gemc (200nM) or irradiated with UV light. After 12-24h treatment, cells were collected, diluted to 2×10^5 cells/ml in PBS. Cells were then mixed with low melting point agarose (1:10), and then placed on a CometSlide (Trevigen). After the gel was solidified at 4°C, the slide was incubated with the lysis solution at 4°C for 1h, then transferred to an alkali solution at room temperature for another 20 min to allow DNA to unwind. After alkali electrophoresis, the slides were dipped in 70% ethanol for 5 min and air dried. The

DNA was stained with SYBR Green I and imaged with the Zeiss Axio Scope fluorescent microscope. Comet tail moments were measured and quantified using the CometScore software. At least 100 cells were measured per treatment.

Immunofluorescence Detection of γ -H2AX Foci. Cells growing in chamber slides (Nunc® Lab-Tek® II) were treated with dox (200 nM) or gemc (50 nM) for 24h. Cells were then fixed in 4% paraformaldehyde for 30 min, permeabilized in 0.2% Triton X-100 for 15 min, and then blocked overnight with 1% BSA at 4^o C. Cells were probed with primary antibodies against phosphorylated H2AX Ser¹³⁹ (Upstate Biotechnology), washed with PBS and probed with Alexa Fluor conjugated secondary antibodies (Molecular Probes). The cells were mounted with 10 μ l of ProLong^(R) Gold antifade reagent with DAPI (Invitrogen). H2AX foci were visualized under the Zeiss Axio Scope fluorescent microscope and were scored using the ImageJ software (v1.47, NIH). At least 100 cells were counted and graded depending on the number of foci per cell.

Recovery Assays. Cells were seeded in 6 cm dish and DNA damage checkpoint was activated by treating cells with 200 nM doxorubicin for 24h. Doxorubicin was washed away and nocodazole was added immediately to the culture medium to prevent their exit from mitosis. Caffeine (5 mM) was also added to inhibit ATR and ATM checkpoint kinases in order to inactivate DNA damage signaling and allow mitotic re-entry. At 24h doxorubicin treatment, 4h and 24h caffeine exposure, cells were collected, fixed in formaldehyde and then stored in 70% ethanol at -20°C overnight. Cells were then stained with phospho-H3 (FCMAB104A4, Millipore) and PI. Mitotic fraction was analyzed by FACS.

Co-immunoprecipitation. 293T cells were transfected with the indicated HOXC10 construct. After 24h, they were treated with doxorubicin or other drugs for an additional

24h. Cells were collected in the EBC lysis buffer (50 mmol/L Tris-HCl (pH 8.0), 120 mmol/L NaCl, 0.5% NP40) supplemented with complete protease and PhosSTOP phosphatase inhibitors cocktails (42). 1 mg of protein lysates were precleared and subjected to immunoprecipitation overnight at 4°C with CDK7 antibody (C-19, Santa Cruz) or normal rabbit IgG control (sc-2027, Santa Cruz). The immune complexes were loaded onto 4% to 12% NuPAGE gels (Invitrogen) and immunoblotted with the following antibodies: Myc-Tag (9B11, Cell Signaling), RNA Polymerase II (CTD4H8, Millipore), and XPD (sc-101174, Santa Cruz).

CDK7 Kinase Activity. Cells were treated with dox (100 nM) or gemc (100 nM) for 24h. Cells were collected in lysis buffer and 300 µg of protein extract was used for immunoprecipitation with CDK7 antibody. The Cdk7 immunoprecipitate was washed three times in lysis buffer, once in kinase buffer (50 mM, pH 7.5, 10 mM MgCl₂, 250 µM EGTA, 10 mM β-glycerophosphate, 1 mM DTT) and resuspended in 40 µl of kinase buffer. Kinase reaction was performed by adding 10 µl of a mixture containing 50 nM ATP and 20 ng GST-CTD peptide (P4016, Proteinone) as the substrate. The reaction was incubated for 1h at 30°C and then an equal volume of kinase-GLO™ reagent (Promega) was added and incubated for another 15 min at room temperature. As control, kinase reaction was performed with the same samples in the absence of the CTD peptide substrate. Luminescence was recorded and expressed as relative RLU to the untreated control cells.

Survival Analysis in Patients with Breast Cancer. Kaplan-Meier analysis was performed by employing an updated version of the online available KM-plotter using 3,999 breast cancer patients <http://kmplot.com/analysis> (47). In brief, to assess the prognostic value of a gene, each percentile (of expression) between the lower and upper quartiles were computed and the best performing threshold was used as the final cutoff

in a univariate Cox regression analysis. Kaplan-Meier survival plots and the hazard ratio with 95% confidence intervals and logrank P value were calculated and plotted in R using the Bioconductor package "survival". Statistical significance was set at $p < 0.01$. Cox proportional hazard regression was performed to compare the association between HOXC10 expression, clinical variables and relapse-free survival using WinSTAT 2007 for Microsoft Excel (Robert K. Fitch Software, Germany).

Statistical Analysis. Results were expressed as mean \pm SEM of at least 3 independent experiments. Paired t-test or ANOVA tests were performed for data analysis, and significant difference was defined as $p < 0.05$. All statistical analyses were performed using GraphPad Prism version 4.03 (GraphPad Software, Inc.).

CHAPTER 3

HOXC10 is preferentially and functionally overexpressed in breast tumors

3.1 HOXC10 mRNA is frequently overexpressed in breast cancer

To obtain a global profile of HOX gene expression in breast cancer, we conducted a tiling array of the 39 genes in the HOX clusters using normal breast organoids (n=4), primary breast tumors (n=8) and breast cancer metastasis to the liver (n=6) (40). HOXC10 was among the top five overexpressed genes in the tumor samples (Figure 3.1a). Mining the online database Oncomine, we found that HOXC10 was consistently among the top 1% of overexpressed genes in breast cancer compared to normal tissues (Figure 3.1b), which is also consistent with previous studies (38, 39). Interestingly, comparing different cancer types, HOXC10 overexpression was not a common feature among all carcinomas, suggesting a unique role of HOXC10 in breast cancer (Figure 3.1c and <http://cgap.nci.nih.gov>). We then validated the microarray data by performing qRT-PCR in a panel of normal breast, invasive carcinoma, and distant metastatic breast tissues (Figure 3.2a), as well as in 50 breast cancer cell lines (Figure 3.2b). We found that HOXC10 overexpression is common in breast cancer and is equally enriched in cell lines and breast cancer tissues regardless of their subtype, ER/PR, HER2 or p53 status.

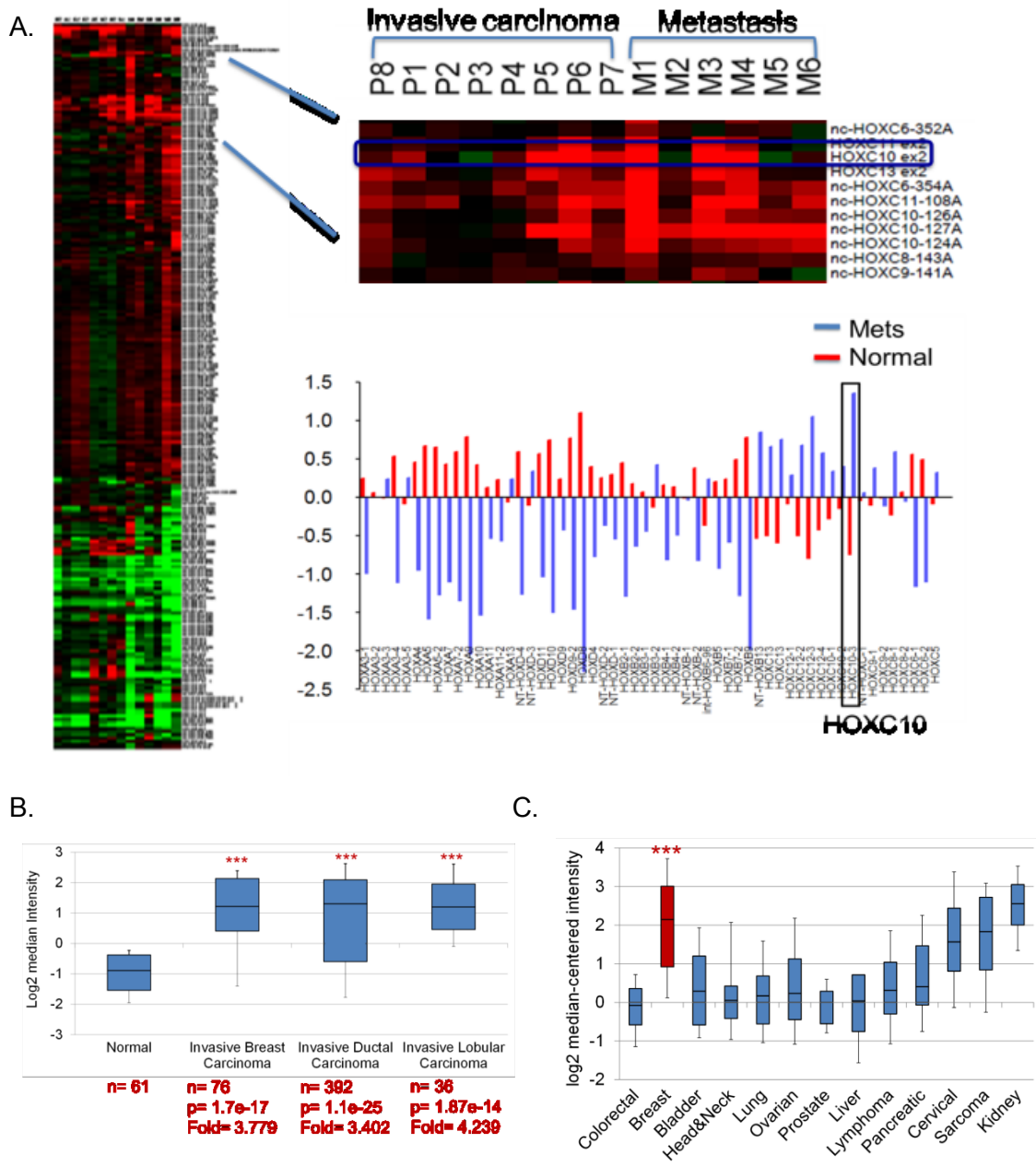
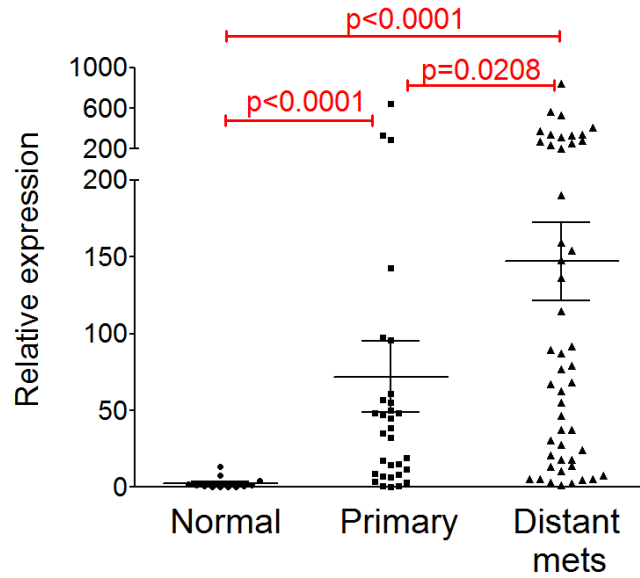


Figure 3.1 Global expression analysis revealed that HOXC10 is commonly overexpressed in breast cancer. A. tiling array of the 4 HOX clusters conducted on 8 breast cancer primary tumors and 6 liver metastasis tissues identify many mis-expressed HOX genes, including HOXC10, and many ncRNAs. (Right panel) A histogram of the average expression of the HOX genes from the tiling array data shows HOXC10 among the highly overexpressed genes in the distant metastatic tissues. B. Data from the TCGA dataset showing that HOXC10 is significantly overexpressed in both ductal and lobular carcinomas of the breast compared to the normal breast tissues. C. Bittner multi-cancer dataset showed that HOXC10 is overexpressed in breast, cervical, sarcoma and kidney cancers, but not in many other carcinomas ($p= 3.18 \text{ e-}40$; t-Test: 14.306; Fold change= 2.387).

A.



B.

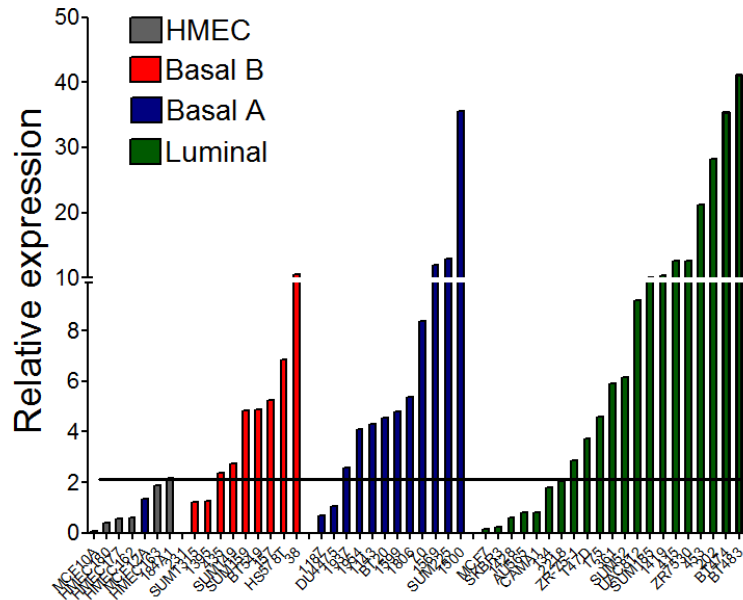


Figure 3.2. Real-time PCR in tumors and cell lines validated HOXC10 overexpression in breast cancer. A. qRT-PCR measurement of HOXC10 expression in a panel of normal breast organoids (n=12), invasive primary carcinoma (n=31) and distant metastatic breast tissues (n=49). Samples were collected through the JH rapid autopsy program. HOXC10 is 10-fold higher in 67% of invasive carcinomas and in 82% of distant metastatic samples. B. qRT-PCR measurement of HOXC10 in 50 breast cell lines divided by their subtypes. HOXC10 was overexpressed in almost 75% of cancer cell lines.

3.2 HOXC10 overexpression increases aggressiveness of cancer cells

To investigate if overexpression of HOXC10 has functional consequences in breast cancer, we stably overexpressed HOXC10 (myc-tagged) in MCF10A-Ras and MDA-MB-231 breast cells. Conversely, HOXC10 was depleted by using specific shRNAs in four cell lines (SUM159, SUM149, MCF7 and HCC1143). Both invasion through matrigel and anchorage-independent growth (number and size of colonies growing in soft agar) were reduced in cell lines with depleted HOXC10 levels (Figure 3.3a and 3.3b). When injected subcutaneously into nude mice, HOXC10 overexpressing MCF10A-Ras-C10 xenografts grew much faster than their vector transfected counterpart, MCF10A-Ras-v. Stable knockdown of HOXC10 in SUM149 and in SUM159 breast cancer cells very significantly suppressed the growth of the xenografts, and their vascularization, implying a dependence on HOXC10 for growth (Figure 3.3c and 3.3d).

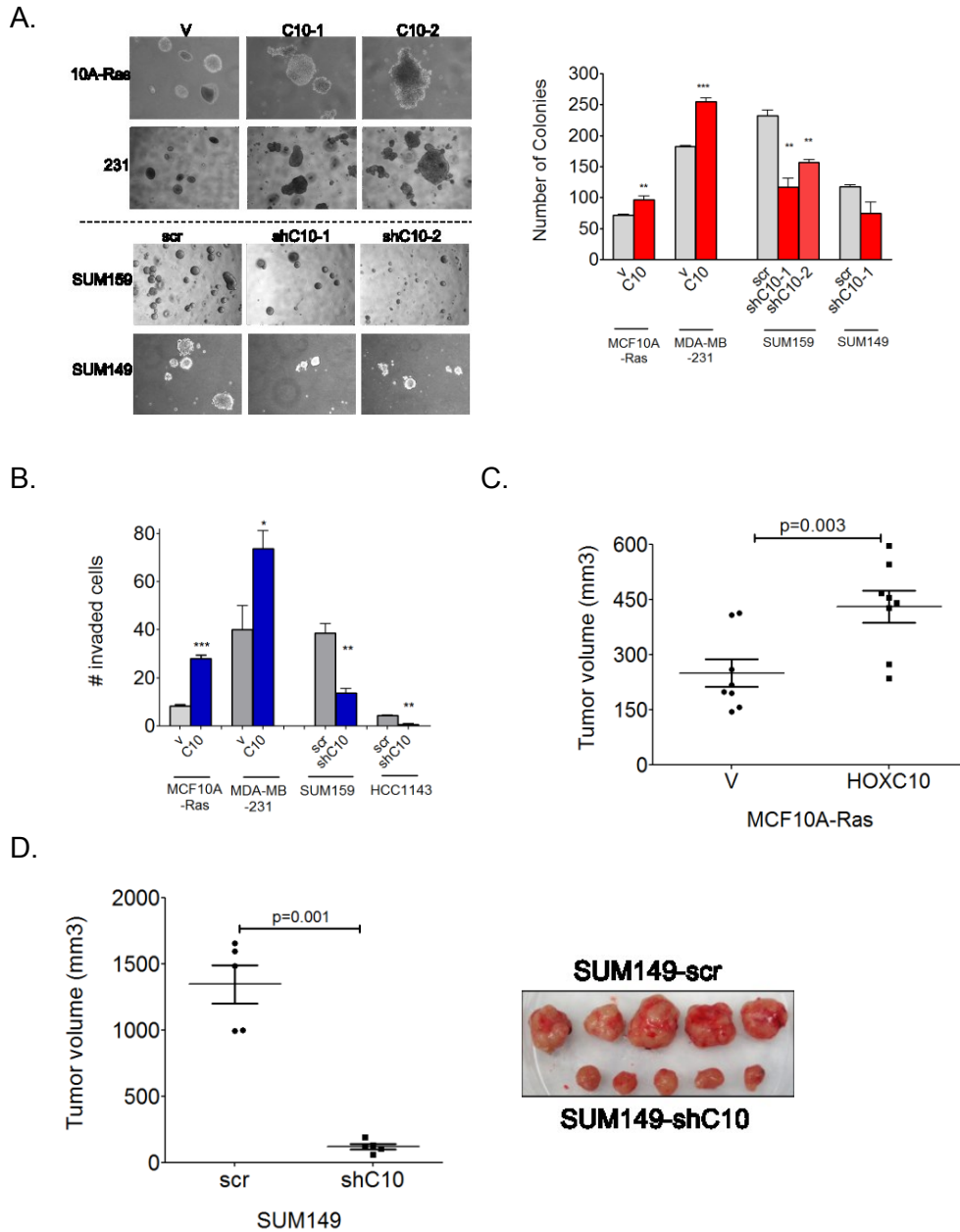


Figure 3.3 High-levels of HOXC10 leads to more aggressive in-vitro and in-vivo phenotypes. A. Representative images of growth in soft agar as colonies (left) and their quantification (right). B. Average number of invading cells through a matrigel coated chambers. (C) MCF10A-Ras-C10 or MCF10A-Ras-vec; and (D) SUM149-shC10 and its control SUM149-scr were injected subcutaneously into nude mice. Size of the tumors 5 weeks later is shown. Representative xenografts of SUM149-shC10 and SUM149-scr are presented on the right (* $p < 0.05$; ** $p < 0.001$; *** $p < 0.0001$).

CHAPTER 4

HOXC10 promotes proliferation by facilitating G1/S transition during cell cycle progression

4.1 HOXC10 increases proliferation of cancer cells

Studies in amphibians and HeLa cells have associated HOXC10 with cell cycle progression, with cell proliferation control and with tissue regeneration; however the underlying mechanism remains largely unknown. In agreement with these purported functions, transient or stable knockdown of HOXC10 in different breast cancer cell lines significantly reduced their proliferative rate by 30-50% (Figure 4.1a, $p < 0.0001$). Conversely, stable overexpression of HOXC10 in MDA-MB-231 cells led to an increased proliferation by 51% (Figure 4.1b). No significant effect on proliferation was observed, however, upon stably modulating HOXC10 levels in SUM159 and MCF-10A-Ras under normal culture conditions. On the other hand, HOXC10 expression in these cells under non-optimal conditions (reduced serum and growth factor) led to a growth advantage, allowing the cells to continue cell division and growth (Figure 4.1c). A deletion construct of HOXC10 lacking the 3rd helix failed to induce increased proliferation in cells, or to recover it after HOXC10 knockdown (Figure 4.2). These data thus indicate that to enhance proliferation, the ability of HOXC10 to bind DNA was required to enhance.

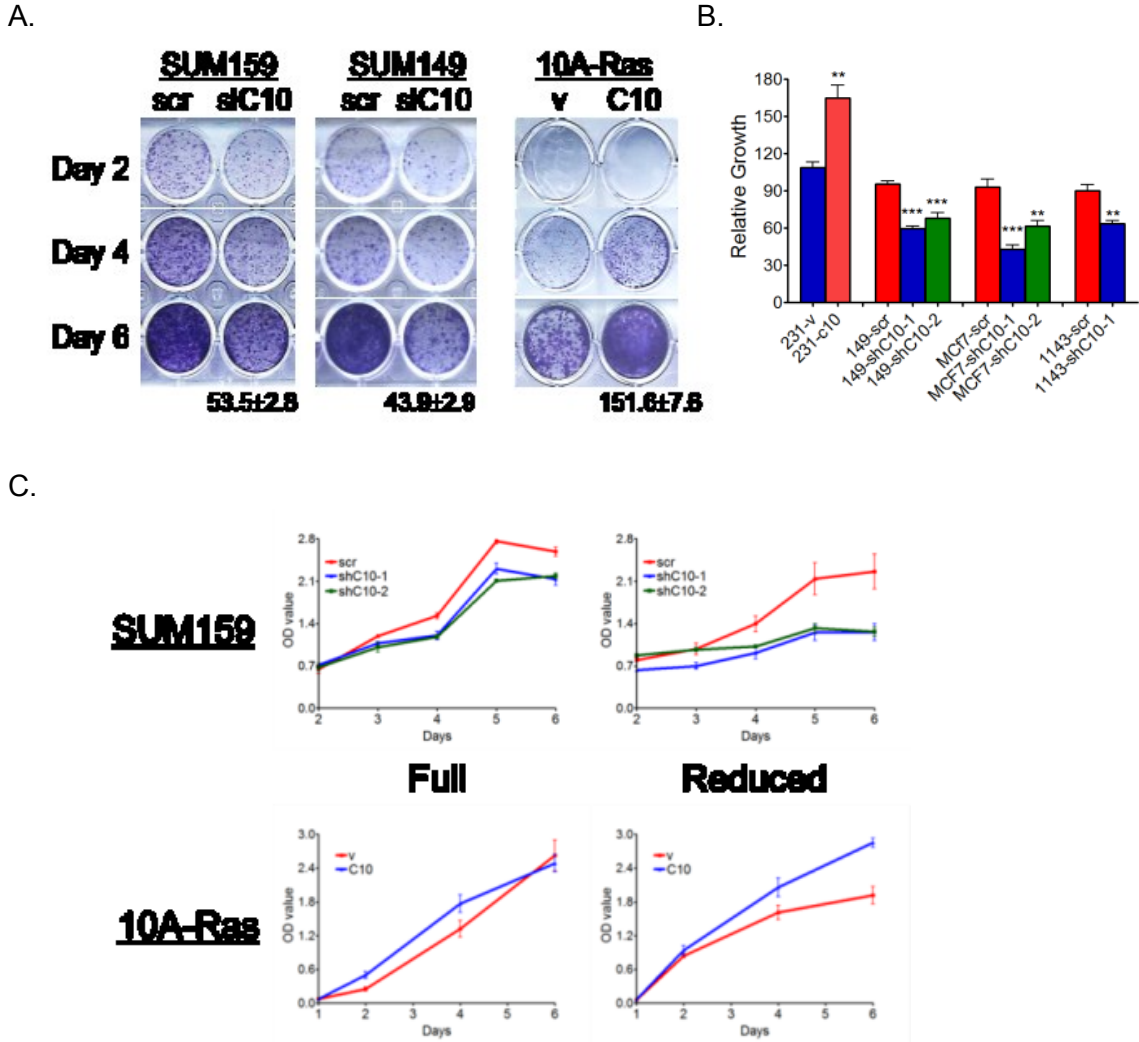


Figure 4.1 HOXC10 promotes the proliferation of cells under optimal and non-optimal conditions. A. HOXC10 was transiently overexpressed in MCF10A-Ras, and transiently knocked-down in SUM159 and SUM149 with siRNA. Cell growth was monitored by crystal violet staining. B. Equal number of cells were seeded, stained with crystal violet after 6 days and quantified (** p,0.001; ***p<0.0001). C. Stable modification of HOXC10 levels affected the growth of the cell lines under reduced serum conditions (0.5%).

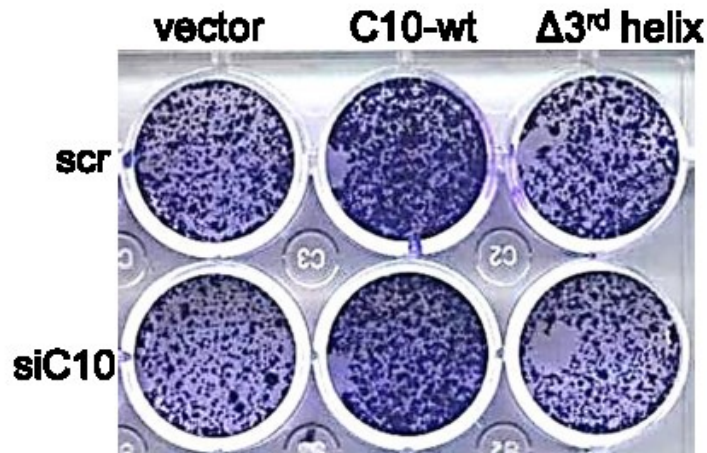
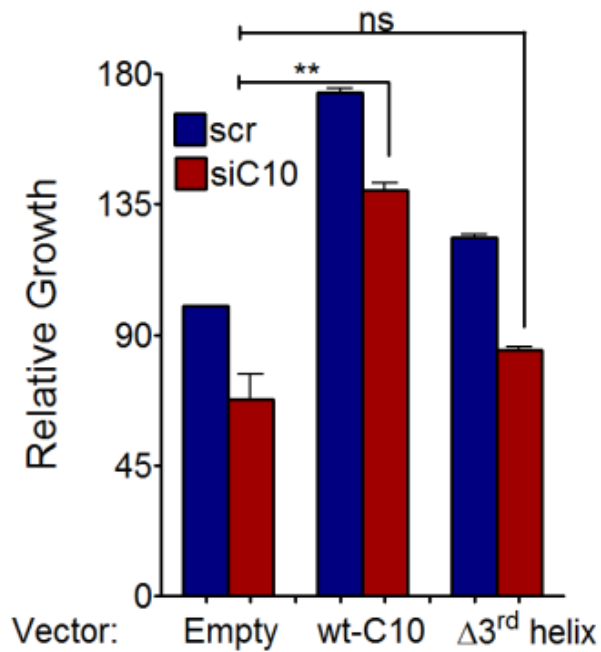


Figure 4.2 HOXC10 DNA binding ability is required for promoting proliferation. MCF7 were treated with scr or siHOXC10. 24h later, the cells were transfected with an empty vector, wild-type HOXC10 or $\Delta 3^{\text{rd}}$ helix mutant. Proliferation was assessed following crystal violet staining.

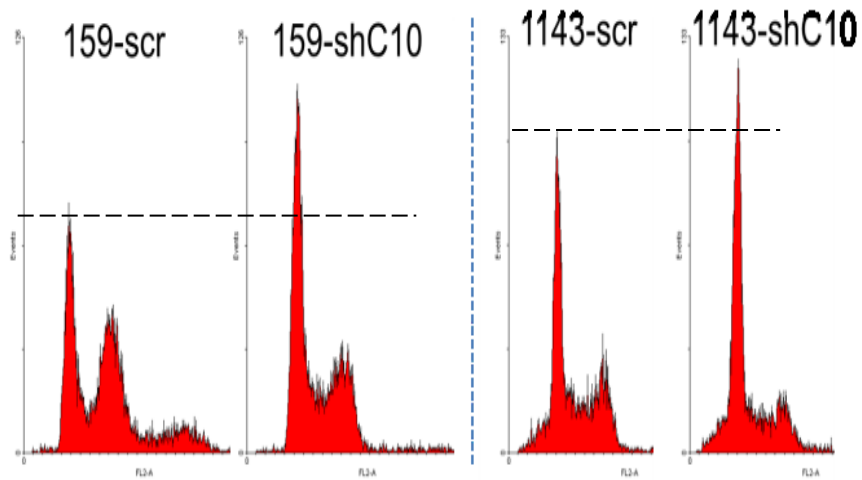
4.2 HOXC10 facilitates G1/S transition

To explore how HOXC10 drives proliferation, we first analyzed the cell cycle distribution. There was a modest increase in G1-phase cells and a decrease in G2-phase cells and polyploidy after HOXC10 knockdown (Figure 4.3a and Table 1). We next examined BrdU staining in unsynchronized cells and found that although the total number of BrdU-positive cells was not affected, their distribution was different: 15-33% more BrdU-positive cells accumulated at late G1/ early S phase upon HOXC10 knockdown (Figure 4.3b). These results are consistent with role of HOXC10 in firing of new origins as single molecule analysis of replication dynamics by DNA fiber analysis (Figure 4.4 A-C) revealed that HOXC10 is required for the initiation of new origins- but not the accumulation of stalled forks after hydroxyurea (HU) treatment. These observations suggest that HOXC10 has a role in G1/S transition. To provide further confirmation, cells were synchronized at G1/S phase by double thymidine treatment. In MCF-7 cells, knockdown of HOXC10 delayed the progression of cells in the S phase by at least 2h (Figure 4.5). In sum, HOXC10 is involved in the early phases of G1/S transition, and is important for the optimal transition of breast cancer cells through the S phase.

	SUM159			HCC1143			SUM149	
	scr	shC10-1	shC10-2	scr	shC10-1	shC10-2	scr	shC10-1
G1	36.9±2.7	51.6±2.1	51.57±0.8	53.1±2.9	59.5±3.3	69.4±3.1	43.5±3.8	50.9±4.4
S	12.6±2.4	23.3±1.7	16.5±1.9	19.4±0.5	16.9±0.4	12.3±1.5	17.7±3.4	17.1±2.5
G2/M	36.2±2.8	21.8±1.1	24.1±0.3	20.2±2.2	17.9±2	10.1±0.8	31.2±1.1	26.7±2.5
>4N	14.1±1.5	2.9±0.4	7.6±0.7	2.4±0.5	3.0±1	2.4±1	6.7±0.5	3.9±0.3

Table 1. Cell cycle distribution. Data shows an enrichment in the G1 phase after stable knockdown of HOXC10 in different cell lines.

A.



B.

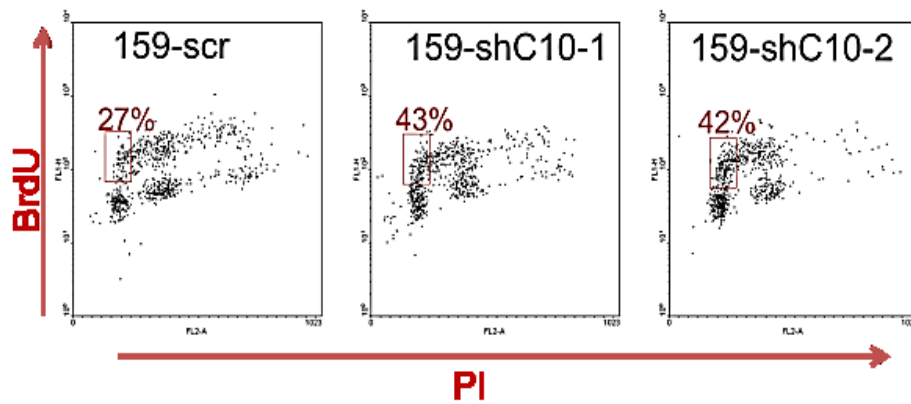
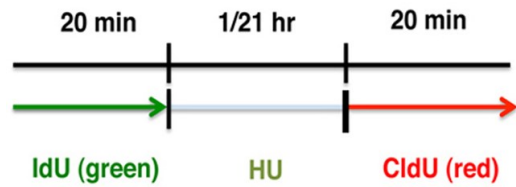
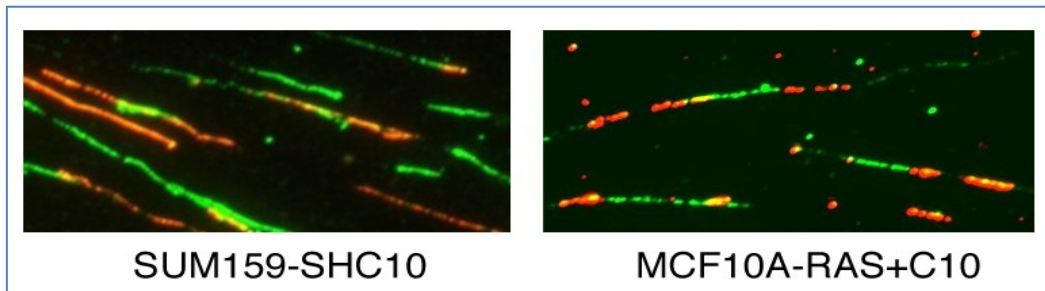


Figure 4.3 Knock-down of HOXC10 arrested cells at late G1. A. Cell cycle profile revealed an arrest of cells at G1 upon HOXC10 knockdown. B. Enrichment at early S phase in HOXC10 knock-down cells as detected by BrdU staining suggests a defect in S phase progression.

A.



B.



C.

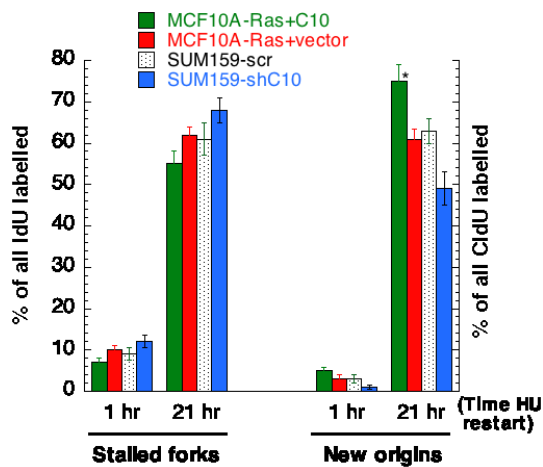


Figure 4.4 Cells failed to start new origins efficiently. HOXC10 is required for the resolution of stalled replication forks as measured by the DNA fiber assay. A. Workflow of the DNA fiber assay. B. Representative images illustrating that most DNA from the HOXC10 knockout cells are stained in green (failed to restart replication) as compared to the red staining DNA from HOXC10 overexpression cells. C. Quantification of the stalled forks and new origins in three replicates.

* Reproduced in collaboration with Dr Tej Pandita, , Southwestern University, Dallas, TX

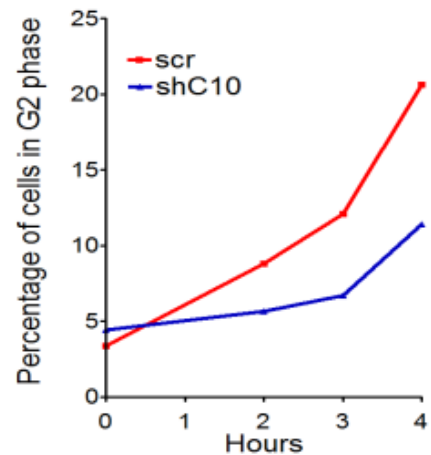
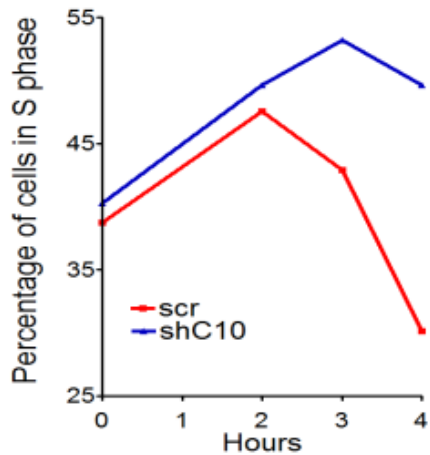
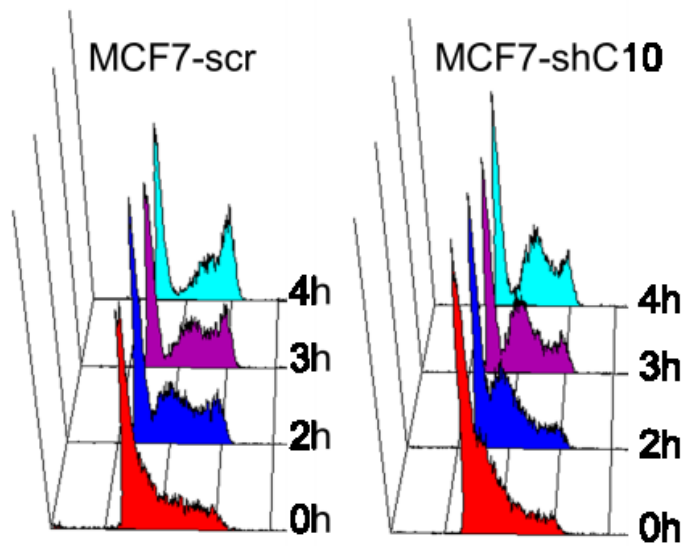


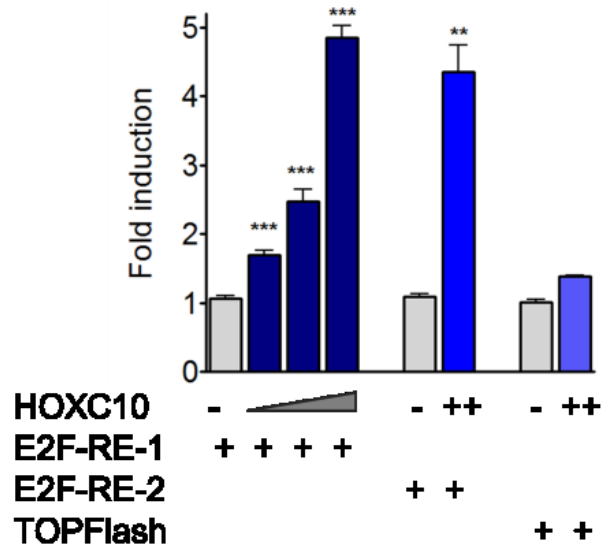
Figure 4.5. Cells exhibit a delayed G1/S transition. MCF7-scr and -shC10 were arrested at late G1 by double thymidine block. After release (0h), the progression of cells through the S phase was monitored by PI staining. The percentage of cells in S or G2 phase is represented below the graphs

4.3 HOXC10 indirectly activates the E2F1 pathway to promote proliferation

Since HOXC10 depletion results in the arrest of cells in G1/S transition and E2F1 is known to regulate the expression of genes involved in the control of the progression from G1 into S phase, we investigated whether HOXC10 regulates the transcriptional activity of E2F. Using a luciferase construct containing E2F-responsive elements cloned upstream of the luciferase reporter gene, we first looked at the effect of HOXC10 on E2F1 transcriptional activity. HOXC10 was able to activate 2 different constructs (DHFR and DNA Pol α promoters) in a concentration- dependent manner when transiently overexpressed in 293T cells (up to 5 fold increase in activity, Figure 4.6A). This effect was specific for E2F as it was not observed in the WNT-responsive construct (TOPFlash). We also observed the same trend in the stable cell line model: A 1.5 fold increase in E2F activity was measured in MCF10A-Ras-C10 versus the vector control, MCF 10A-Ras-v; and conversely, a 1.5 fold decrease was detected in SUM159-shC10 compared to SUM159-scr (Figure 4.6B). We speculate that the difference in the extent of the fold increase observed between the two sets of cell lines in Figure 4.6A and 4.6B is mainly due to the difference in efficiency of transfection in these cell lines. HOXC10 DNA-binding ability was required for this effect, since only the deletions in the homeodomain or in the 3rd helix failed to activate the E2F-responsive construct (Figure 4.7). We surmise that E2F1 activation was indirect since there was no evidence of physical interaction between HOXC10 and E2F1 (data not shown). To confirm the luciferase data, we measured the expression of a panel of genes defined as the breast cancer “cell proliferation signature”, several of which are also known E2F1 targets. The gene list includes TTK, MCM7, CDC6, PLK1, BUBR1, MAD2, and CENPA. As predicted, there was a significant (25-40%) decrease in the overall expression of these genes upon the depletion of HOXC10 in SUM159-shC10 and HCC1143-shC10, and a 26% increase

in MCF10A-Ras-C10 cells stably overexpressing HOXC10 (Figure 4.8A). The effect was even more pronounced in tumors of the MCF10A-Ras cell lines grown as xenografts (Figure 4.8B). Finally, higher levels of the hyperphosphorylated (inactive) pRB, pCDK2 (active), Cyclin A and Cyclin D confirmed the activation of the E2F pathway at the G1 and S phases (Figure 4.9). Collectively, these data show that HOXC10 is important- though not through direct interaction- for the activation of E2F1 pathway, promoting continuous proliferation.

A.



B.

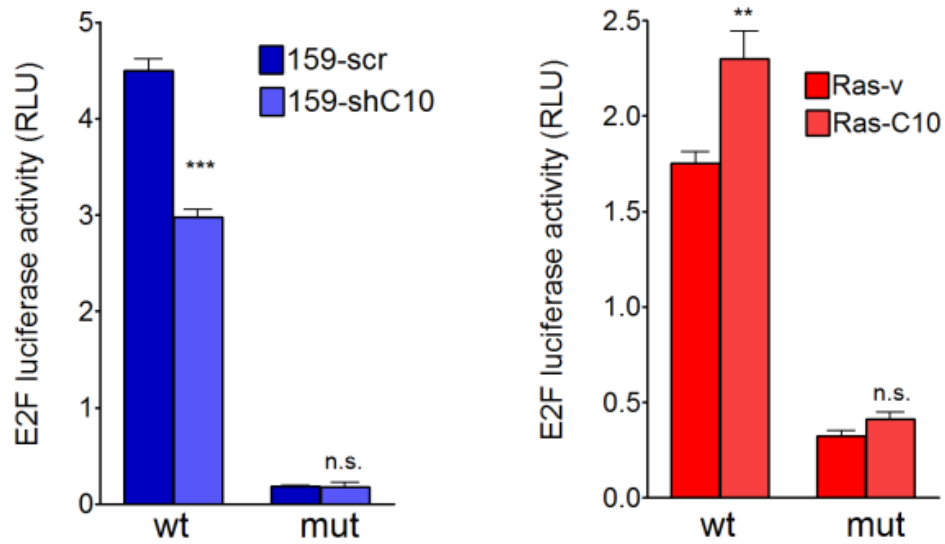
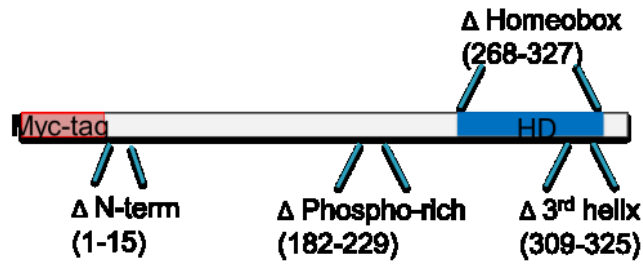


Figure 4.6. HOXC10 activates E2F1 transcriptional activity. A. 293T cells were transiently transfected with HOXC10 expression vector along with a luciferase construct with E2F-responsive element (DHFR promoter: RE-1; Pol II α promoter: RE-2), or WNT responsive element (TOPFlash). Luciferase activity was measured 48h later. B. E2F activity is higher in the stably HOXC10-expressing cells. Cell lines were transfected with E2F wt or mutant responsive element (RE) construct, and luciferase activity was measured.

A.



B.

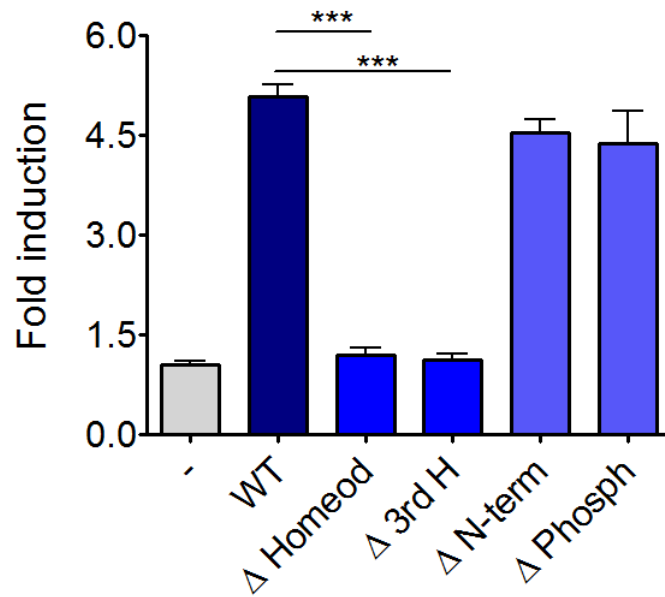


Figure 4.7. HOXC10 transcriptional ability is required for E2F1 activation. A. 293T were transfected with different HOXC10 deletion constructs (as depicted in the drawing) along with E2F-RE luciferase. B. Marked reduction of luciferase activity with delta homeodomain and delta 3rd helix constructs indicates that HOXC10 DNA-binding ability is necessary for E2F activation.

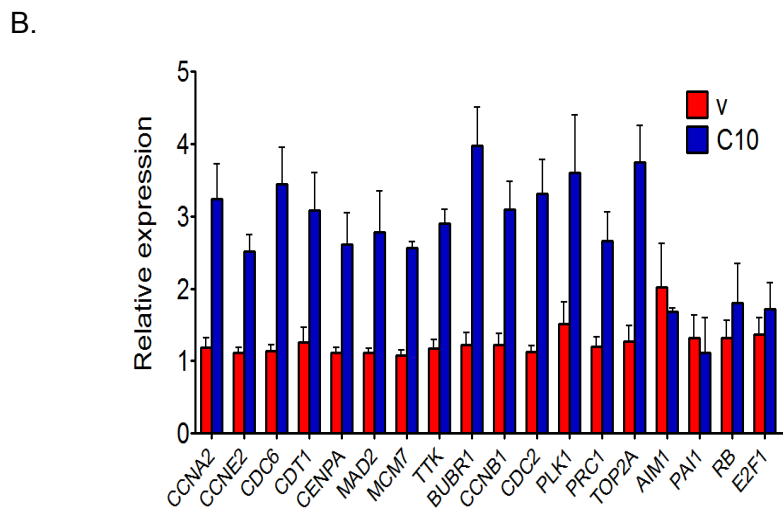
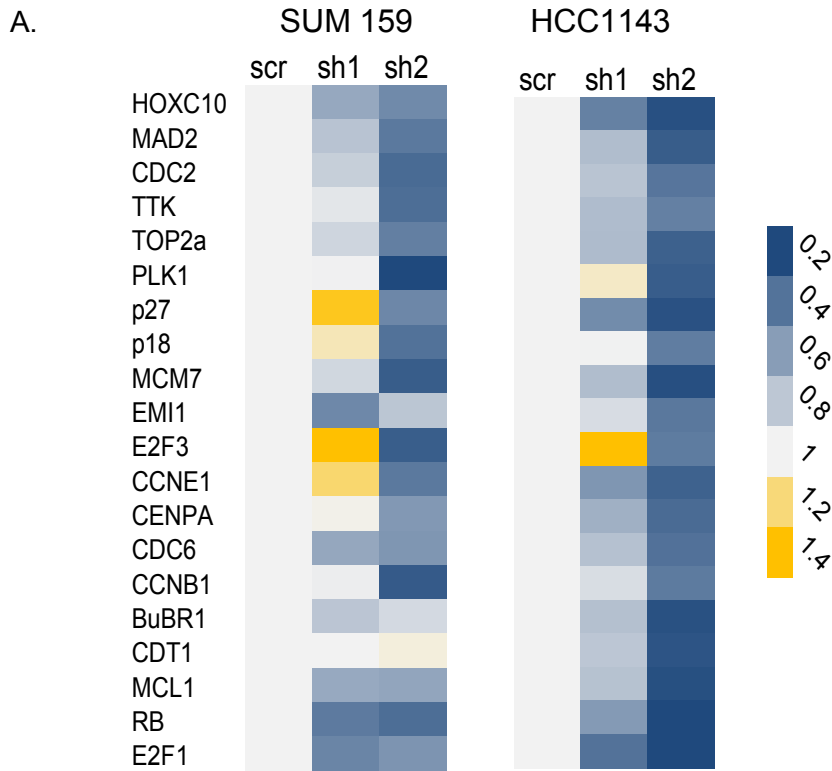


Figure 4.8. The cell proliferation signature genes are expressed at higher levels in the presence of high HOXC10. A. Many genes in the breast cancer cell proliferation signature were downregulated upon HOXC10 depletion (qRT-PCR measurement) in SUM 159 and HCC 1143 breast cancer cells. B. MCF10A-Ras-C10 xenografts had a higher cell proliferative signature than their empty vector counterparts. Pooled expression of all the genes is shown on the right. (*p<0.05; **p<0.001; ***p<0.0001).

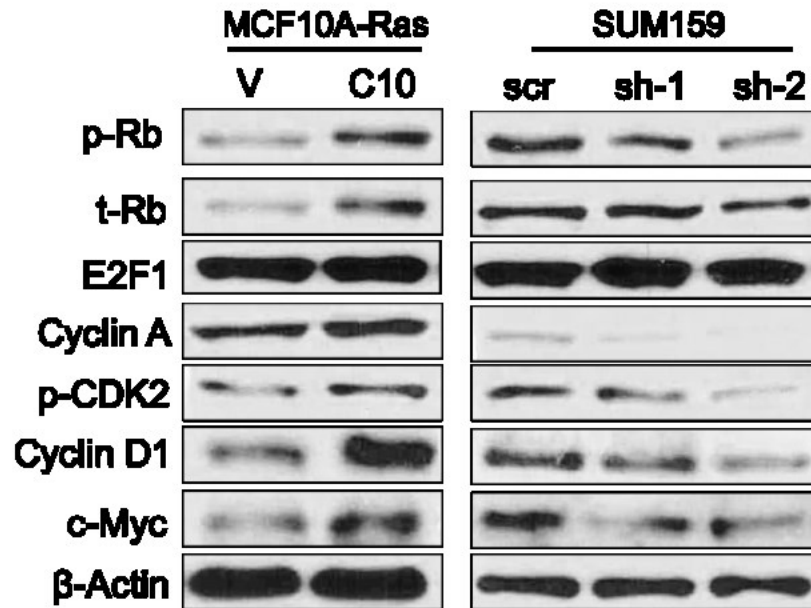


Figure 4.9. Higher protein level or activity of cell cycle proteins validated the RT-qPCR data. Western blot analysis of the levels of some proteins involved in the progression from G1 to S phase.

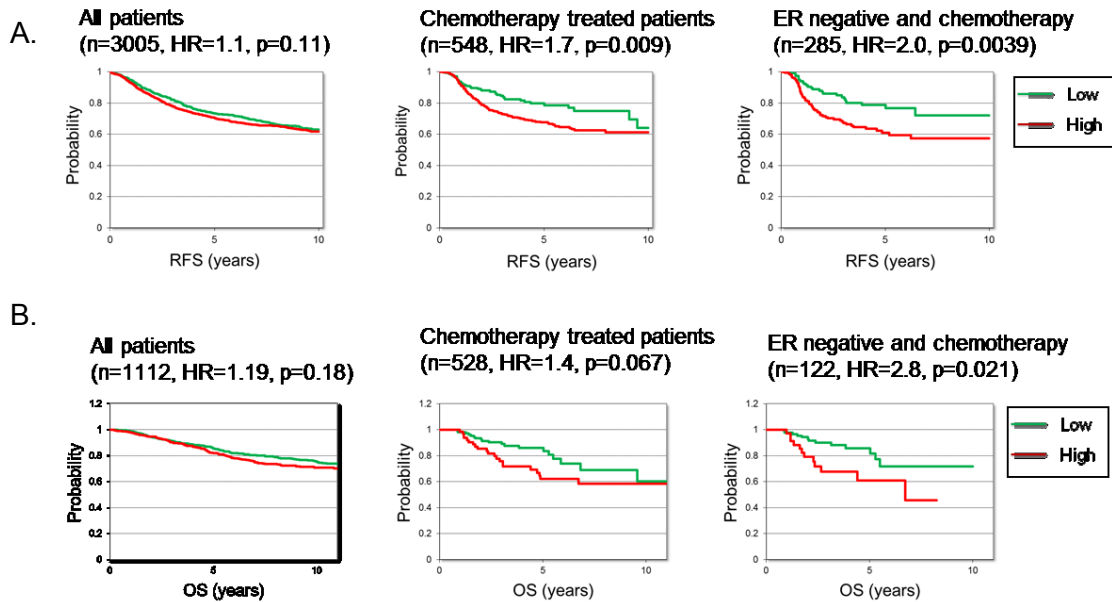
CHAPTER 5

HOXC10 actively promotes chemotherapy resistance and its expression after treatment predicts poor prognosis

5.1 High levels of HOXC10 correlates with poor prognosis in treated patients

Given that the proliferation and E2F gene signatures (7-9, 13) and many HOX genes (27, 28, 48, 49) had been previously shown to be correlated with survival in breast cancer, we next studied if the expression HOXC10 has a prognostic value for assessing the future course of the disease.

Interestingly, analysis of data downloaded from GEO or from the METABRIC cohort showed that HOXC10 expression is prognostic only not in all patients but only in patients treated with chemotherapy- for both relapse-free survival (RFS) and overall survival (OS) (Figure 5.1A, 5.1B). This becomes more substantial in ER/PR negative- treated patients. The significance is retained ($p=0.00014$) in Cox multivariate regression analysis including known clinical parameters (HOXC10, ER, HER2, lymph node status, grade, age and Ki67 expression). Of note, HOXC10 had the highest significance ($p=0.00014$) after the inclusion of all other parameters (Figure 5.1c). When using a ROC analysis, HOXC10 was predictive for response to anthracycline-taxane based chemotherapy regimens ($n=974$, $p=4.7e-04$, $AUC=0.571$).



C. Cox regression in chemotherapy treated patients

	Coefficient	Conf. (±)	Std.Error	P	Hazard = Exp(Coeff.)
218959_at	0.000214095	0.000130885	6.67784E-05	0.001345973	1.000214118
ESR1 expression on array	-6.4378E-05	4.7593E-05	2.42823E-05	0.008019912	0.999935624
HER2 expression on array	-2.50816E-06	2.33633E-05	1.19201E-05	0.833345139	0.999997492
Lymph node status	0.637741507	0.507754195	0.259059885	0.013826036	1.892202523
Grade	0.288681801	0.367781043	0.187644564	0.123938614	1.334666972
Age	0.022281756	0.016154682	0.008242236	0.006864325	1.022531849
MKI67 expression on array	0.000163305	0.000701688	0.000358006	0.648280437	1.000163319

Cox regression in all patients

	Coefficient	Conf. (±)	Std.Error	P	Hazard = Exp(Coeff.)
218959_at	3.71983E-05	9.23196E-05	4.71021E-05	0.429681483	1.000037
ESR1 expression on array	-2.76279E-05	1.79027E-05	9.13407E-06	0.002488872	0.999972
HER2 expression on array	1.38078E-05	1.35871E-05	6.93222E-06	0.046390426	1.000014
Lymph node status	0.429874935	0.189282137	0.096573124	8.90041E-06	1.537065
Grade	0.203696609	0.152760533	0.077939535	0.008961517	1.225926
Age	0.007371313	0.008152332	0.004159379	0.076358956	1.007399
MKI67 expression on array	0.00035607	0.000338037	0.000172469	0.038966434	1.000356

Figure 5.1. HOXC10 expression has negative prognostic value in chemotreated patients. A-B. High HOXC10 levels was significantly associated with worse relapse free survival (RFS) and OS in chemotherapy treated breast cancer patients, especially the ER-negative patients, but has no prognostic significance in all patients. C. Cox multivariate regression analysis was made for all patients and for chemotherapy treated patients for HOXC10, ER, HER2, lymph node status, grade, age and MKI67 expression.

* Reproduced in collaboration with Dr. Balazs Gyorffy, Semmelweis University, Budapest, Hungary

5.2 HOXC10 is induced during chemotherapy resistance

Given the clinical data indicating HOXC10 as a marker for poor prognosis in breast cancer, we next investigated how HOXC10 overexpression related to acquired resistance to chemotherapy. First, we measured HOXC10 expression in chemotherapy-resistant MCF7 sublines (41). These sublines were established by a progressive exposure to a drug (epirubicin, paclitaxel or docetaxel), and display 815-, 535- and 251-fold increase in their resistance to each drug, respectively. HOXC10 expression was 2-6-fold higher in the resistant cells (Figure 5.2A). This increase is functional since reducing HOXC10 levels in the Tax-R cell lines restored their response to taxol treatment (Figure 5.2B). Functional redundancy in HOX gene function is often invoked to minimize the effect of one HOX gene, often being studied in isolation. Interestingly, when we examined the expression of some of the other HOX genes in these sublines, we noticed that the expression of genes flanking HOXC10 (i.e. HOXC9 and HOXC11) was downregulated, other genes showed no change (HOXB7 and HOXB13), whereas its paralogs (HOXA10 and HOXD10) were also upregulated (Figure 5.2c). This argues against a redundant function of the HOX genes in general during chemotherapy response, and warrants further investigation of the promoter region of the HOXC10 paralogs.

As in-vivo models are more relevant to human cancer therapeutics, we next measured the level of HOXC10 in de novo chemo-resistant xenografts. We therefore extracted RNA from MDA-MB-231 and SUM159 xenografts in animals treated with doxorubicin or carboplatin. These xenografts at the time of collection had shown regression temporarily, and then resumed their growth during continued exposure to the drugs. In line with the in-vitro model, HOXC10 level was at least 2-fold higher in the surviving MDA-MB-231

(Figure 5.3). Although there was a slight trend for an increase in HOXC10 expression in SUM159, it was not significant. Importantly, SUM159 already have high basal HOXC10 expression levels. The fact that SUM159 xenografts responded poorly to chemotherapy provided additional evidence that HOXC10 could serve as a predictive marker for response.

Finally, we investigated if HOXC10 expression was induced upon short-term chemotherapy treatment. Unfortunately, we could not find a good antibody to detect endogenous HOXC10 protein or its nuclear distribution in breast cancer cell lines, so we limited our work to measuring mRNA. After short-term treatment with different drugs, there was a progressive increase in HOXC10 mRNA levels over days of treatment (Figure 5.4). The induction was most prominent in MDA-MB-231 which has very low basal HOXC10 levels. Collectively, these results suggest that HOXC10 expression is correlated with long-term treatment failure and chemoresistance, and that the protein might be involved in the latter stages of survival in breast cancer.

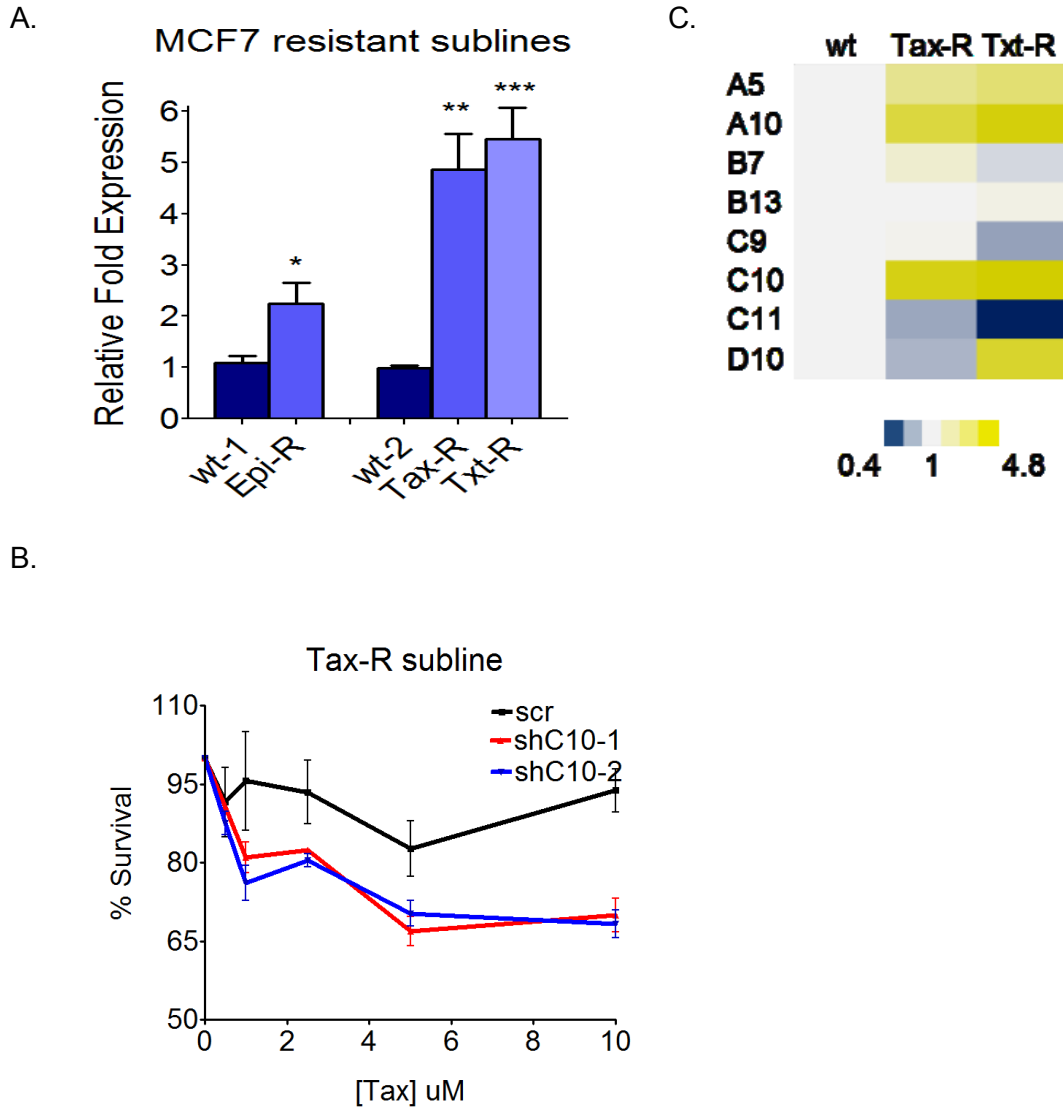


Figure 5.2. HOXC10 expression is functionally induced in an in-vitro resistance system. A. MCF7 chemo-resistant cell lines were established by continuous exposure to epirubicin (Epi-R), taxol (Tax-R) or docetaxel (Txt-R) (31). HOXC10 expression was detected by qRT-PCR. B. HOXC10 was stably depleted in the Tax-R subline by 2 different HOXC10 shRNA. The resensitization of these cells to taxol was measured by MTT. C. Different HOX gene expression was detected by qRT-PCR in the Tax-R and Txt-R MCF7 sublines and supports the notion that upregulation of HOXC10 during chemoresistance is not a common feature of all the HOX genes.

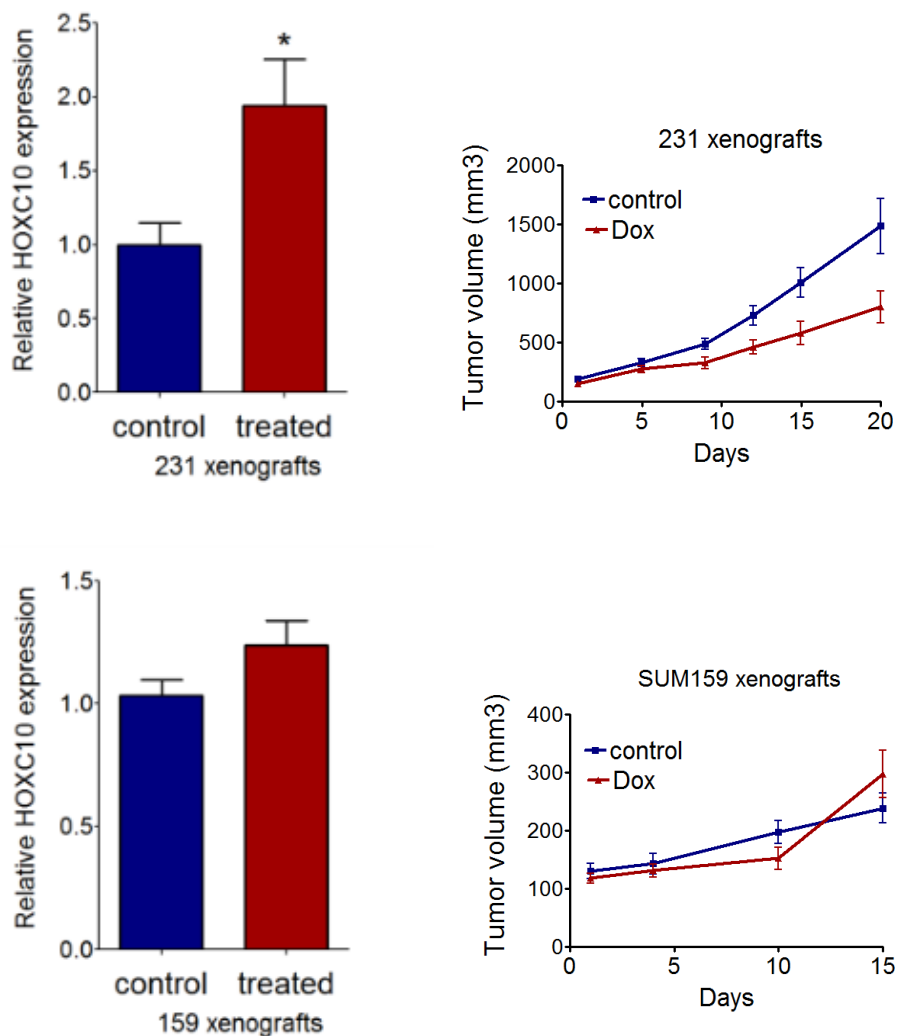


Figure 5.3. De novo induction during therapy or endogenous high HOXC10 expression renders tumors resistant to chemotherapy. HOXC10 expression is significantly increased in MDA-MB-231 xenografts- and not in SUM159 xenografts- treated with doxorubicin or carboplatin. After 2-3 weeks of continuous treatment, surviving tumors were collected and RNA was extracted for qRT-PCR. Tumor growth over the course of treatment is shown on the right.

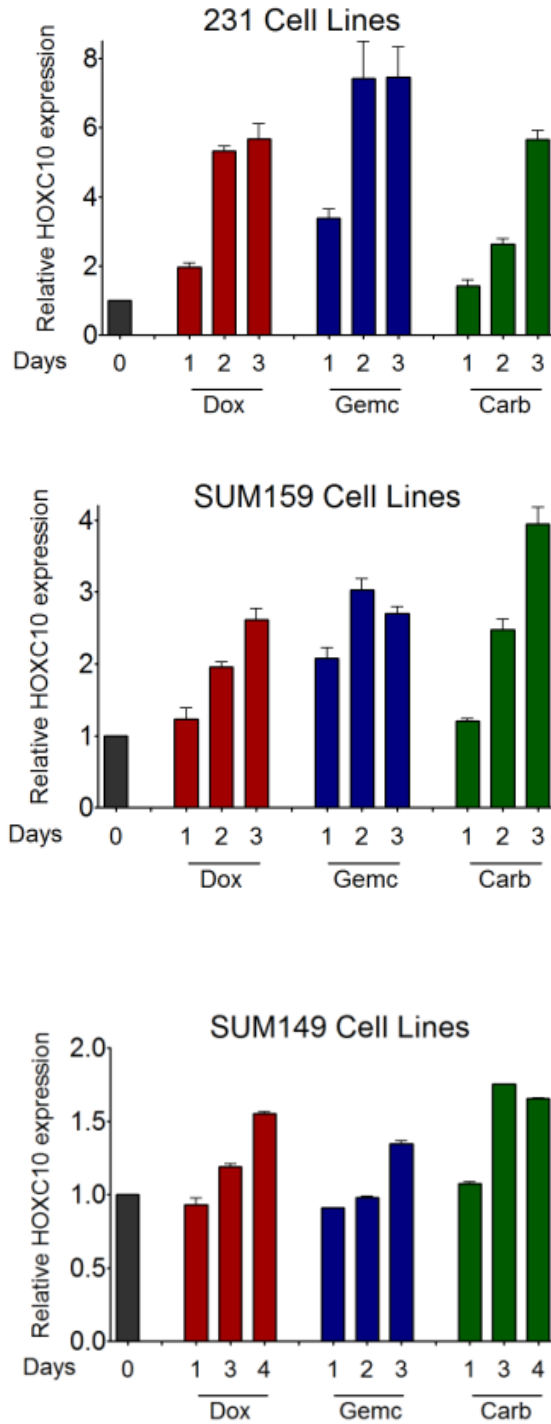


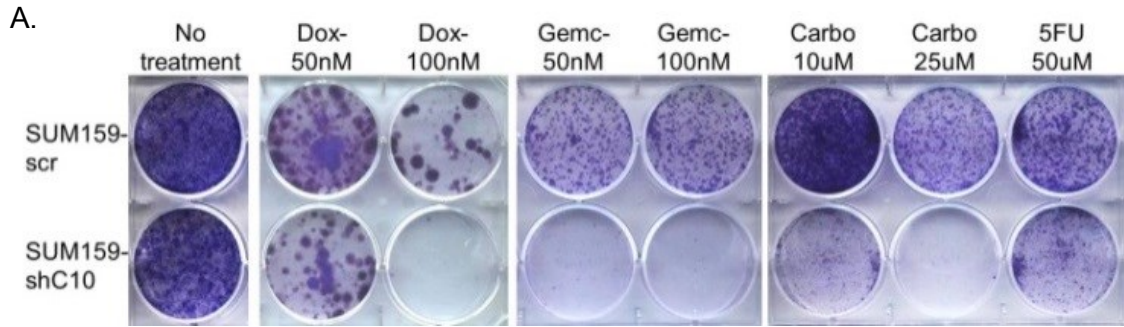
Figure 5.4. HOXC10 expression is induced after short-term treatment of cells in culture with chemotherapy. Induction of HOXC10 expression over days during exposure to chemotherapy in MDA-MB-231, SUM159 and SUM149.

5.3 HOXC10 overexpression decreases susceptibility to chemotherapy treatment.

Given the above data on correlation of high HOXC10 with resistance to chemotherapy in several models, we next focused on investigating the molecular basis of HOXC10 function in decreasing the susceptibility of breast cancer to chemotherapy treatment.

Stable downregulation of HOXC10 in SUM159 (p53 mutant), MCF7 (p53 wt) or SUM149 (BRCA1 mutant) increased susceptibility of these cell lines to different chemotherapeutic drugs, (doxorubicin, gemcitabine, taxol or carboplatin) as measured by colony survival (Figure 5.5) or by MTT (Figure 5.6A). Conversely, MCF10A-Ras-C10 showed a reduced response compared to MCF10A-Ras-v to most of the drugs tested (Figure 5.5, 5.6B). One explanation could be differences in the apoptotic response of the cells. Indeed, there was a slight yet consistent increase in Caspase3/7 activity and in the sub-G1 population in the HOXC10 depleted cells (SUM159-shC10 and MCF10A-Ras-v) as compared to the HOXC10 expressing cells (SUM159-scr and MCF10A-Ras-C10) (Figure 5.7). Further, the expression of many anti- and pro-apoptotic genes was modulated at the protein level, RNA or both (Bid, BCL2, FLIP, BIRC2, BIRC3, HSP27 and BCL-xL) upon chemotherapy treatment (Figure 5.8, 5.9). It is important to note that exogenously modulating HOXC10 levels in different breast cancer cell lines did not affect the baseline apoptotic activity or the expression of most of the apoptotic genes involved (Figure 5.9). The in-vivo data confirmed the above results: Initially, all MCF10A-Ras xenograft tumors treated with doxorubicin stopped growing. By the 3rd weekly treatment, the control MCF10A-Ras-vector tumors reduced in size. On the other hand, MCF10A-Ras-C10 tumors stopped responding to treatment after the 2nd dose of the drug, and eventually resumed their growth. Notably, reflecting this resumption, the tumors showed efficient upregulation of expression of anti-apoptotic genes (Figure 5.10).

Given that the anti-apoptotic genes examined are known direct targets of the NF- κ B pathway, we next measured the activity of NF- κ B in the cells using the NF- κ B-responsive reporter Igk2-IFN-LUC, with and without doxorubicin treatment. Not only the basal activity of NF- κ B was higher in MCF10A-Ras-C10 (overexpression system) and SUM159-scr (KD system) compared to their counterparts, but also after treatment, the difference in luciferase activity was even more pronounced (Figure 5.11). This finding is in agreement with a recent report that the basal activity of NF- κ B is much higher, and maintained as such in doxorubicin-resistant MCF7 cells (50). Of note, the increase in survival could not be attributed to differences in drug accumulation since doxorubicin uptake and retention was similar in the cell lines tested (Figure 5.12). Collectively these data indicate that HOXC10 activates NF- κ B under stress conditions, thus allowing the cells to survive through upregulation of the anti-apoptotic pathway. The E2F pathway was not involved in the response to chemotherapy, as measured by luciferase activity (data not shown), indicating that HOXC10 might be modulating different pathways under normal and stress conditions to support growth and survival.



B.

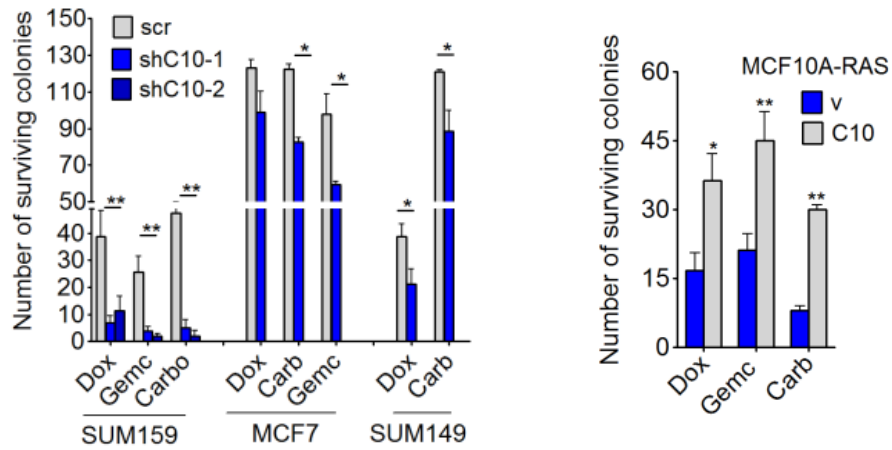
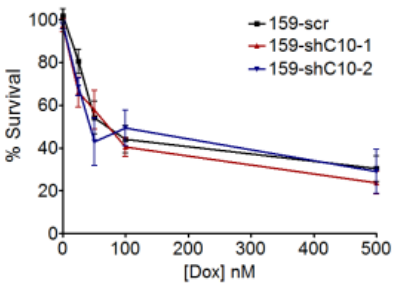
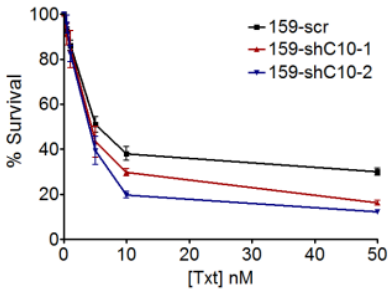
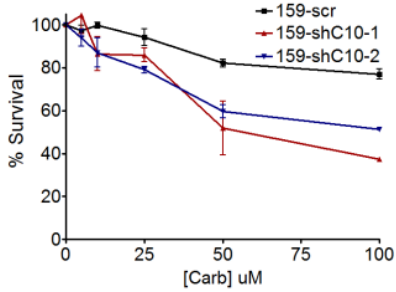
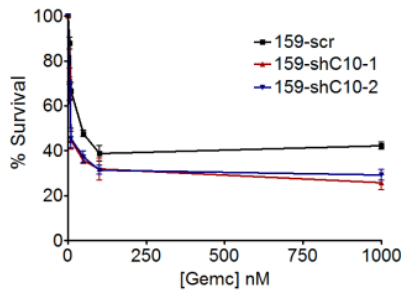


Figure 5.5. Loss of HOXC10 increases log-term drug susceptibility. Representative data (A) and quantification (B) of colony survival assay in cells after different drug treatments.

A.



B.

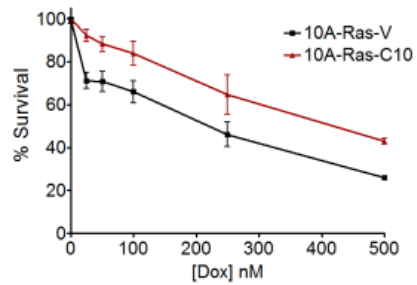
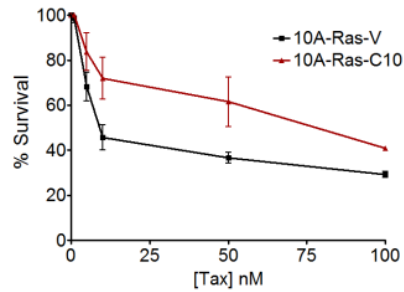
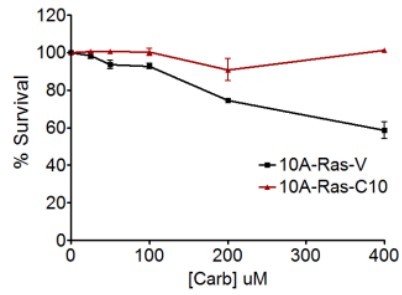
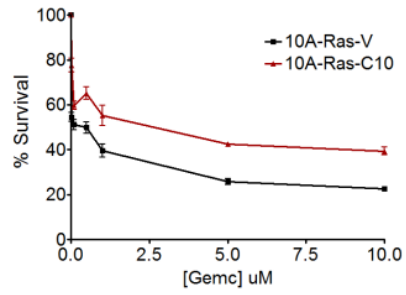


Figure 5.6. HOXC10 modulates short-term drug susceptibility. MTT assay after 48h of chemotherapy treatment in SUM159 (A) and MCF10A-Ras (B) models.

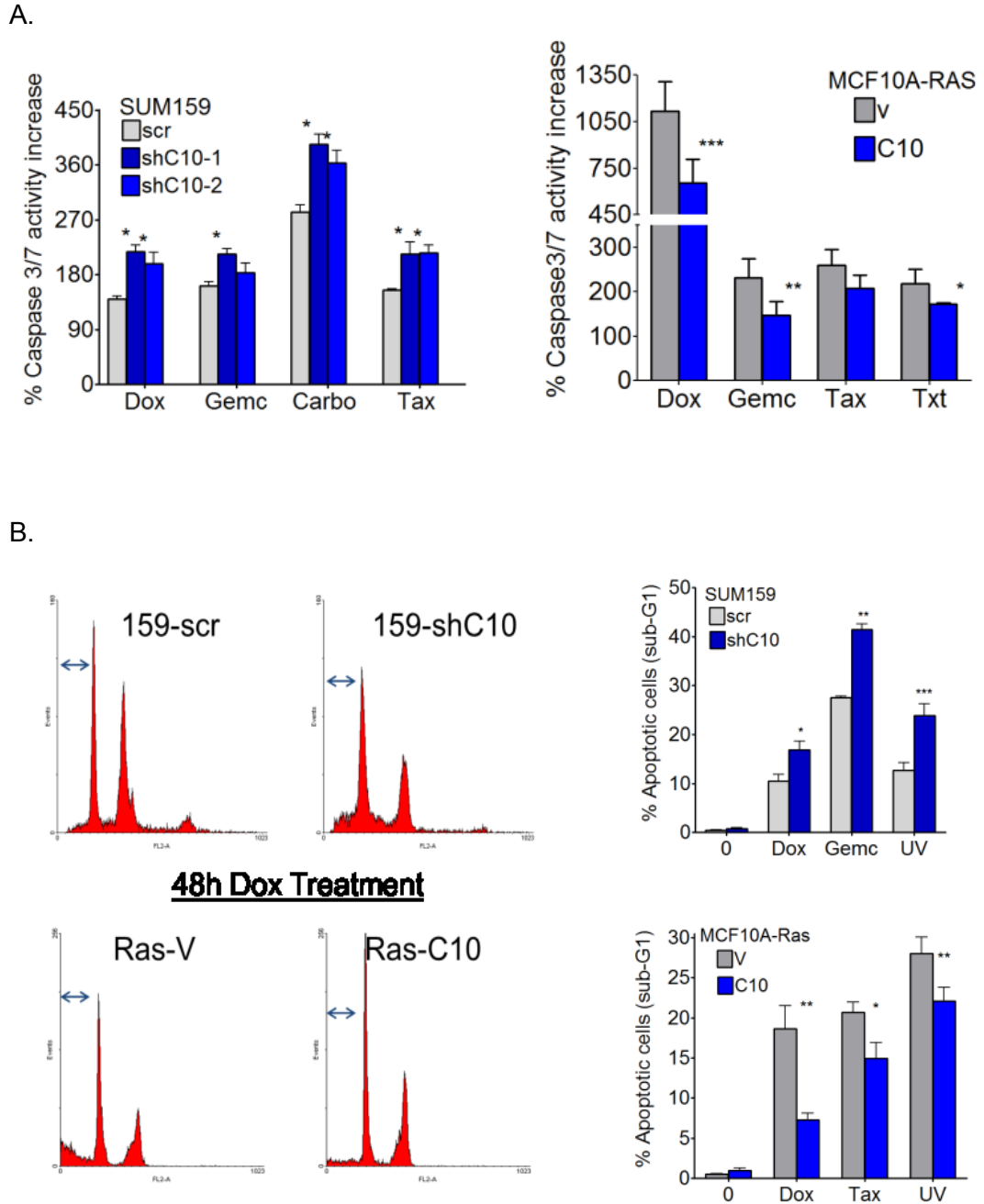


Figure 5.7. HOXC10 decreases apoptosis. HOXC10 decreases apoptosis as measured by caspase 3/7 activity (A) and quantification of cells in sub-G1 (B).

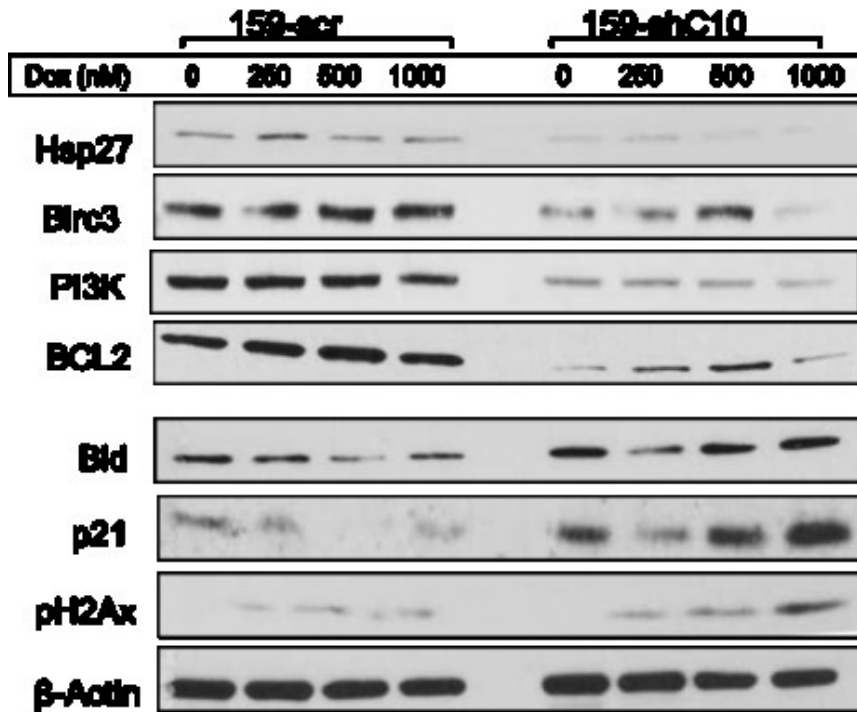
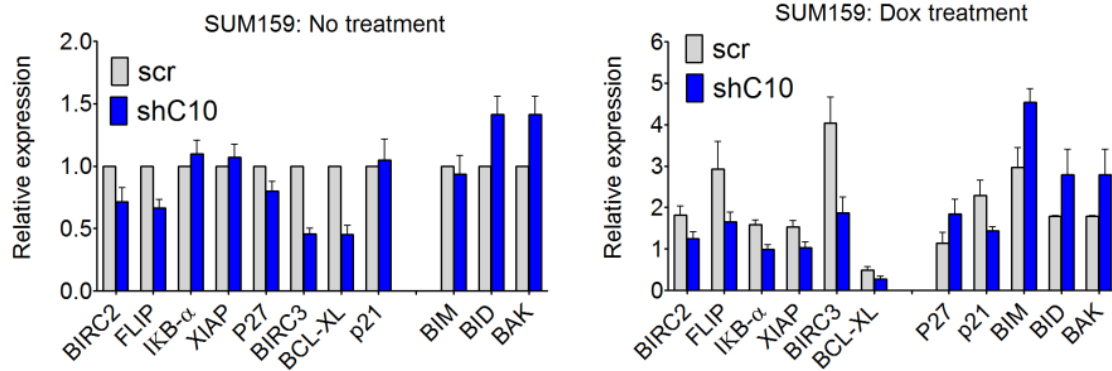


Figure 5.8. HOXC10 decreases apoptosis as measured by levels of the proteins in this pathway. SUM159 cells were treated with different concentration of doxorubicin for 24h. The levels of some pro- and anti-apoptotic proteins were analyzed by western blot.

A.



B.

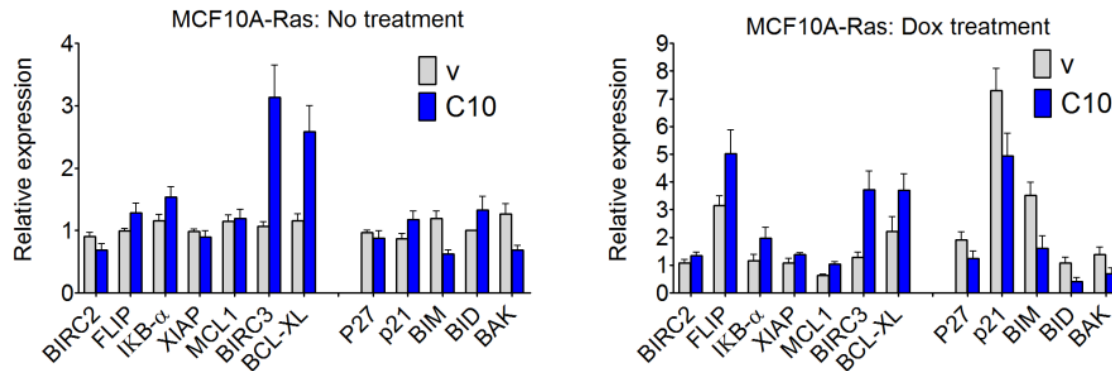


Figure 5.9. HOXC10 decreases apoptosis as measured by levels of the genes in this pathway. SUM159 (A) and MCF10A-Ras (B) were treated with 0 or 200nM doxorubicin for 72h. The expression of some pro- and anti-apoptotic genes was measured by qRT-PCR.

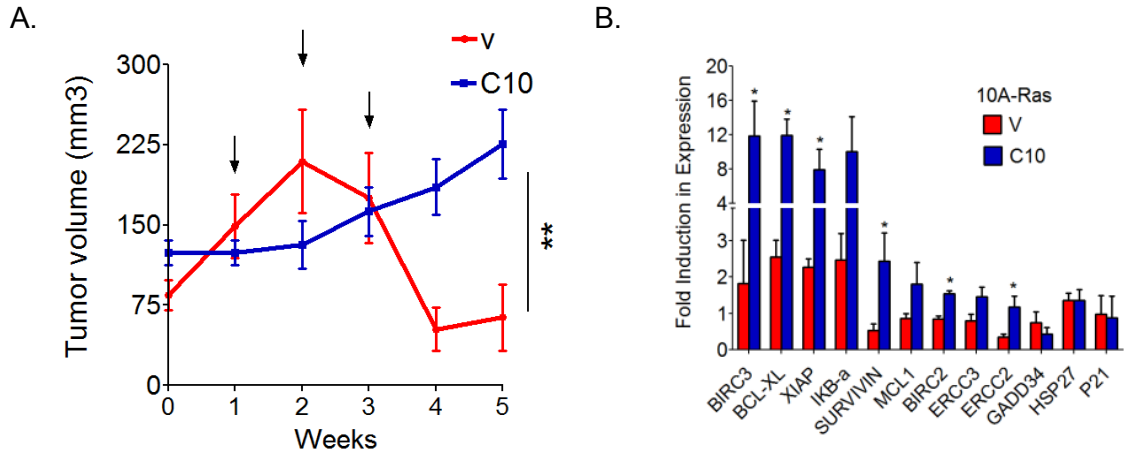


Figure 5.10. HOXC10 protects cells from doxorubicin in-vivo. Xenografts of MCF10A-Ras vector control (n=6) or overexpressing HOXC10 (n=9) were established in nude mice, and mice were treated x3 with 4mg/Kg doxorubicin. Arrow indicates time of treatment. Tumor growth was monitored over weeks (A). Mice were then sacrificed and the expression of many anti-apoptotic genes was measured by qRT-PCR (B).

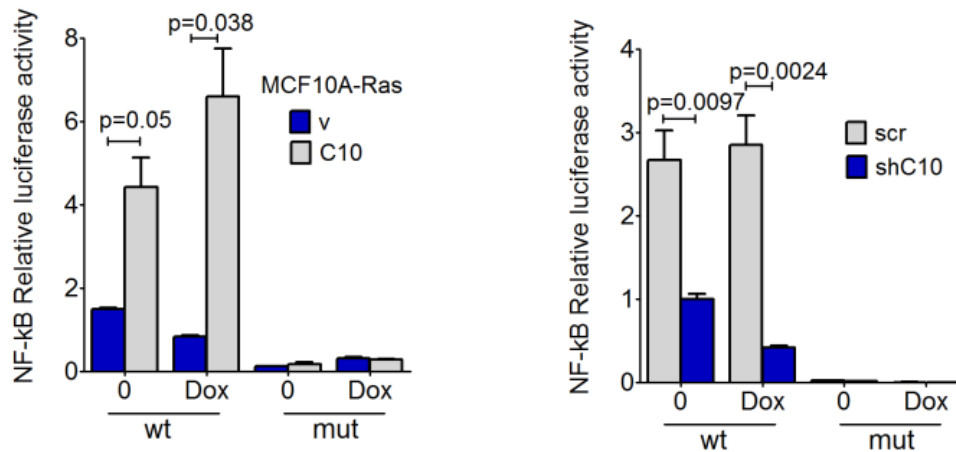


Figure 5.11. HOXC10 increases baseline and induced NF-κβ activity. Cell lines were transfected with NF-κβ wild-type (wt) or mutant responsive element construct. Doxorubicin was added after 24h and luciferase activity was measured 24h later.

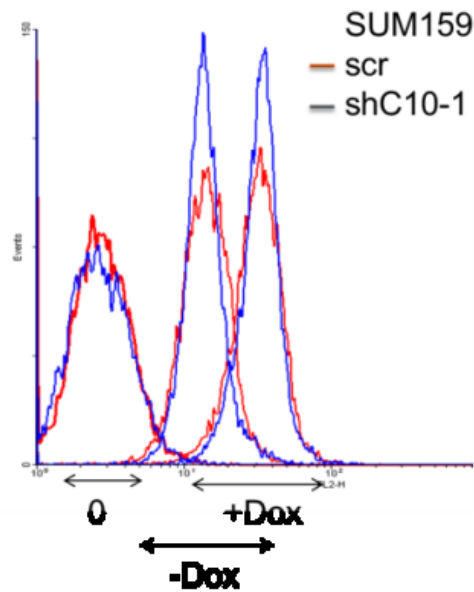


Figure 5.12. No difference in doxorubicin accumulation or retention is observed. Cells were treated with 200nM. After 4h, doxorubicin was washed away. Cells were collected either after 4h of dox treatment (+Dox) or after 4h of dox removal (-Dox) and run directly on flow cytometry.

5.4 HOXC10 stimulates DNA damage repair and checkpoint recovery to promote long-term survival

Since a member of the HOX family proteins, HOXB7, was previously shown in our lab to interact with components of the NHEJ complex promoting DNA double-strand break repair (51), we investigated if HOXC10 could also modulate the DNA repair process. To test this concept, a host-cell reactivation assay was used. Here, the ability of the cells to in-vivo repair damaged luciferase constructs can be quantified by measuring luciferase activity (52). Upon knockdown of HOXC10, there is a significant decrease in repair of DNA crosslinks and adducts introduced to the construct by ultraviolet light or cisplatin pretreatment (Figure 5.13). There was no difference in repair of DNA double-strand breaks (generated by the restriction enzyme Hind III), suggesting that NHEJ pathway might not be affected by HOXC10. Given that the nucleotide excision repair (NER) pathway is mainly involved in repair of DNA crosslinks, and that the most dramatic effect on survival was with treatments with the platinum drugs and with UV light (Figure 5.14), we focused on measuring the activity of the NER pathway by the alkaline comet assay (53). As illustrated in Figure 5.15, upon HOXC10 knockdown, there was significantly more DNA damage after 24h of treatment, leading sometimes to cell death (compare both the shape and DNA content of the tail in the different cells, which are reflected by the tail moment quantification in the graphs below the figures). Further, time-course analysis after UV treatment showed that while DNA damage in SUM159-scr has returned to its baseline levels, it was still 4 fold higher in SUM159-shC10, revealing an inefficient DNA repair in these cells. Each of these findings was confirmed in the overexpression system, MCF10A-Ras-C10 cells (Fig 9).

Phosphorylation of histone H2AX is a surrogate marker of DNA repair efficiency by NER (especially when the drug-induced damage does not involve primarily dsDNA breaks)

(54, 55). We therefore quantified the number of residual γ H2AX foci after 24h of initial treatment. As shown in Figure 5.16, there was on average 20-30% more foci accumulating in SUM159-shC10 after chemotherapy treatment (left), and with almost 50-60% more cells displaying at least 100 foci/nucleus (right). Interestingly, time-course analysis showed no differences in the initial induction of phospho-H2AX (10min-8h) after UV or chemotherapy (Figure 5.17). This is in accordance with reports showing that the residual γ H2AX measured 24 h after treatment- and not the initial kinetics of γ H2AX formation- was a better predictive of cell viability (56, 57). These results indicated HOXC10 might be involved at the DNA damage repair step and not in the checkpoint activation pathway. Examining the DNA damage sensors confirmed that: no major differences in the phosphorylation/activation of the key players in the ATR/ATM pathways were observed (Figure 5.18).

Finally, we examined the possibility that HOXC10 was required for cell-cycle re-entry following DNA-damage-induced arrest. We therefore treated cells with doxorubicin for a short time, and then monitored the percentage of cells that re-entered mitosis after caffeine addition. As Figure 5.19 shows, in the absence of HOXC10, cells were defective in restoring their growth. This highlights the fact that HOXC10 is likely required for checkpoint recovery, besides its role in DNA repair.

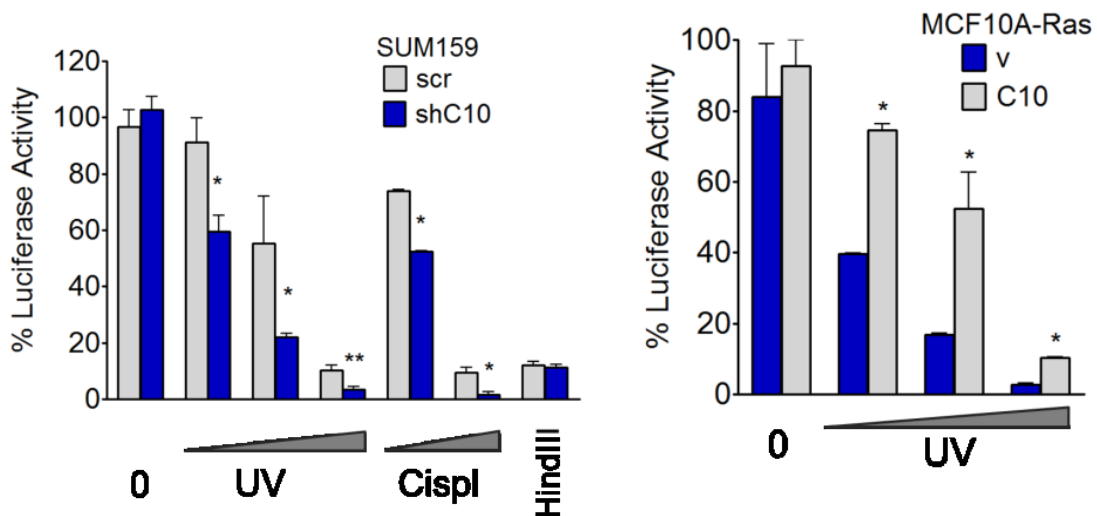


Figure 5.13. HOXC10 activates DNA repair in response to DNA crosslinks. pGL3-basic construct was pretreated with different doses of UV light or cisplatin, or digested with HindIII. Treated vector was transfected into cells and luciferase activity was measured 48h as an indicator of DNA repair.

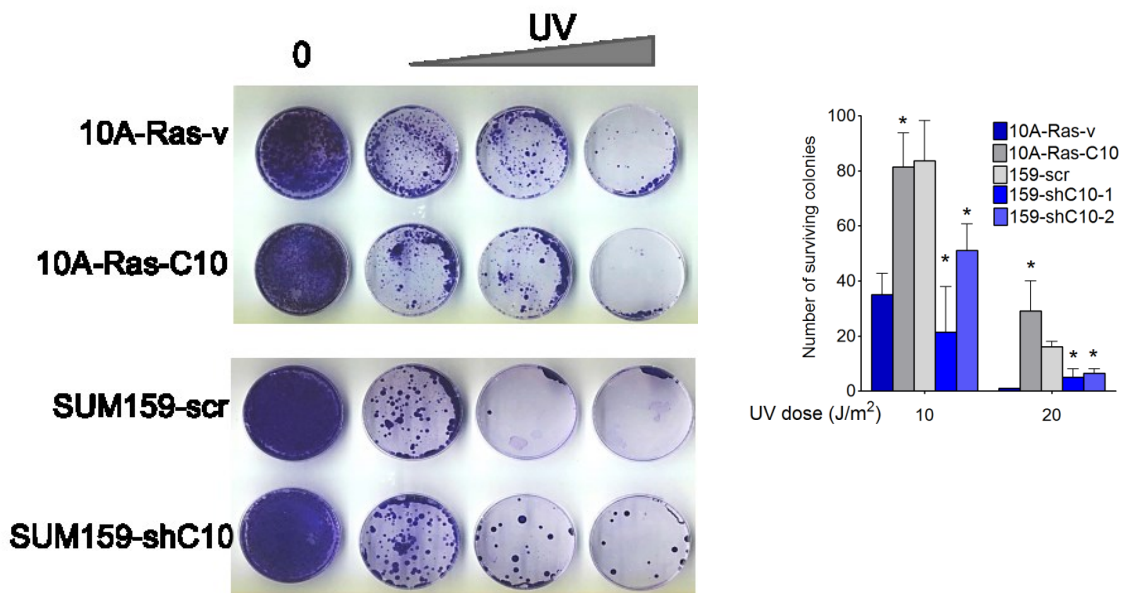


Figure 5.14. HOXC10 effectively protects cells from UV exposure. Representative image of the colony survival assay and its quantification 7 days after initial UV exposure.

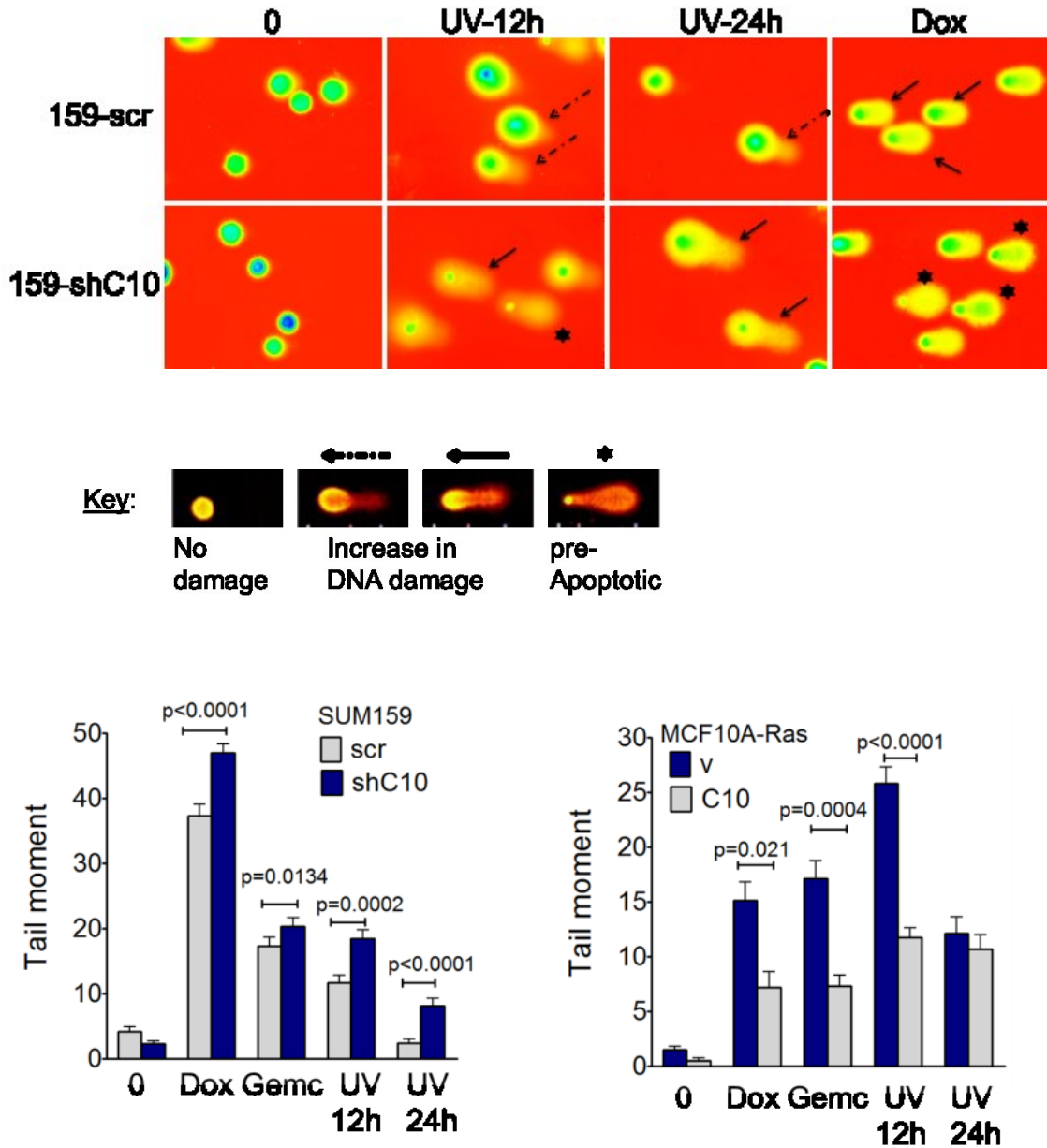


Figure 5.15. Comet assay shows a correlation between efficient DNA repair and expression of HOXC10. Representative images from the alkaline comet assay showing an increase in DNA damage in HOXC10 knockdown cells as illustrated by the length and shape of their DNA tail. Quantifications of the tail moment are depicted in the graphs below.

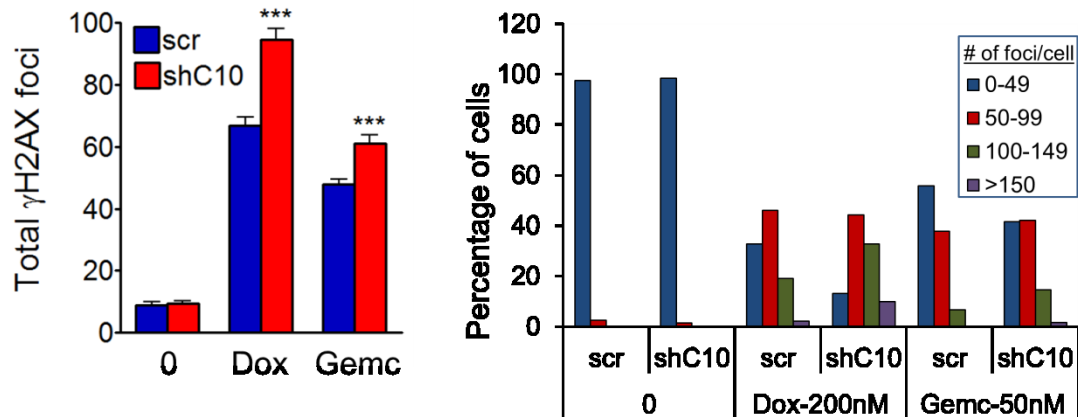


Figure 5.16. More residual DNA damage is observed in the absence of HOXC10 as measured by γ H2Ax foci. Cells were treated with doxorubicin or gemcitabine for 24h. γ H2Ax foci were stained and quantified using ImageJ software. Average number of foci in >150 nuclei is shown in the left graph. Percentage of cells with the noted numbers of γ -H2AX foci is presented on the right and shows that more cells with >150 foci accumulate in the HOXC10- knockdown cell line.

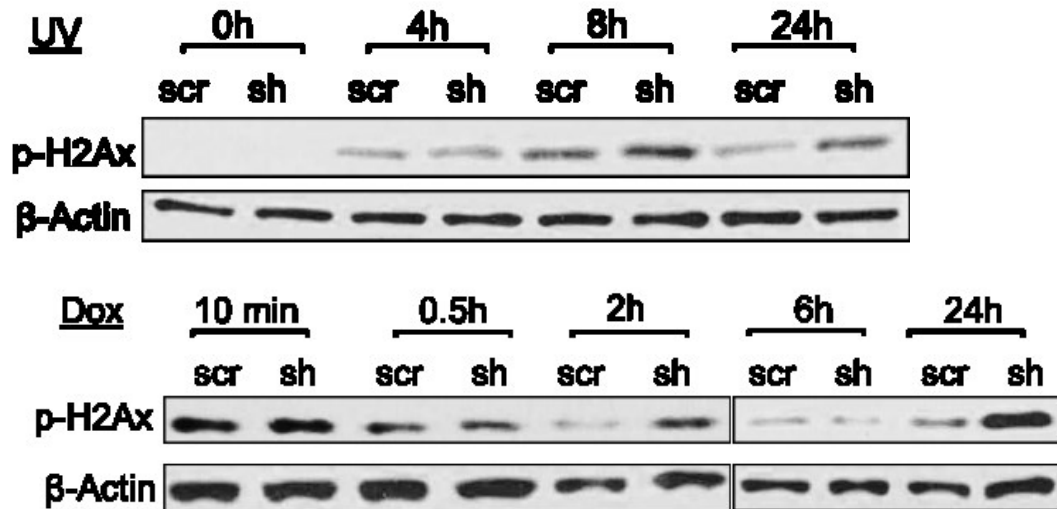


Figure 5.17. No difference in the kinetics of DNA damage induction is observed. SUM159-scr and -shC10 were treated with 200nM doxorubicin or with UV light. Protein was extracted at the indicated time, and the kinetics of H2Ax phosphorylation was monitored by western blot.

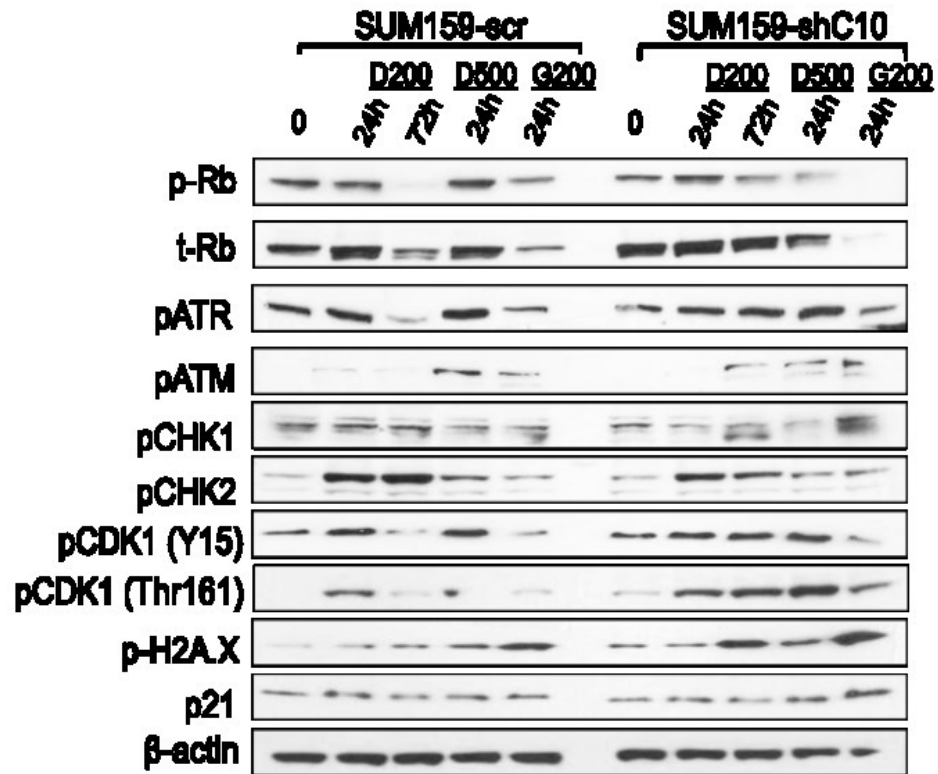


Figure 5.18. HOXC10 does not modulate initial DNA damage response. SUM159-scr and -shC10 were treated as indicated. The activation of proteins in the ATM/ATR pathways was detected by western blot.

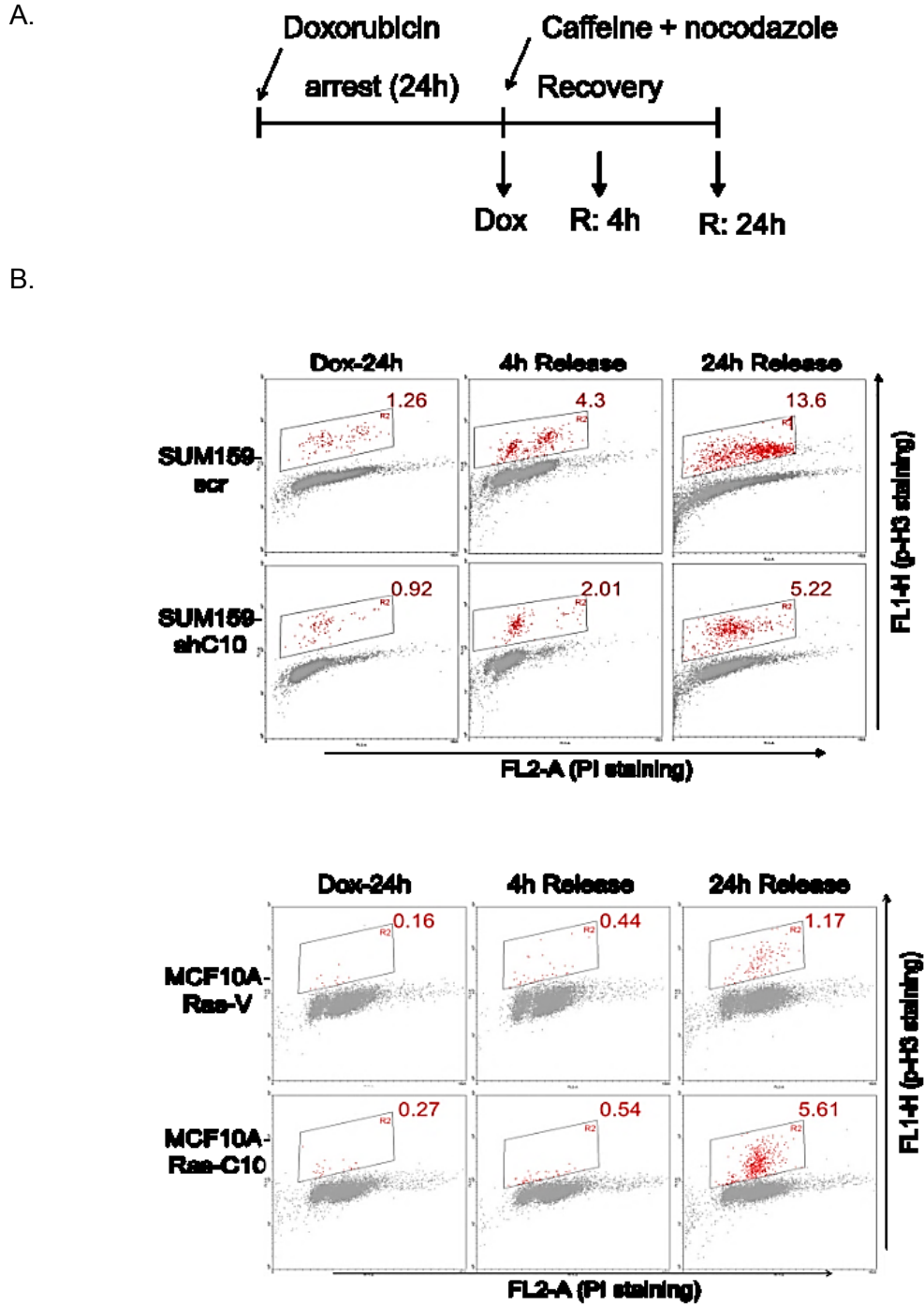


Figure 5.19. HOXC10 is required for efficient checkpoint recovery. A. Schemae of the recovery-induced experimental setting. Cells were collected at the indicated time, and the amount of mitotic cells was determined by pH3 positivity by FACS (B).

CHAPTER 6

HOXC10-CDK7 interaction: a new model and target for chemoresistance

6.1 HOXC10 binds to CDK7 in vivo after chemotherapy treatment

How does HOXC10 affect apoptosis, NF- κ B activity and DNA-damage repair (mainly by the NER pathway)? One key protein that links all three pathways is CDK7. In fact, using a yeast four-hybrid system to identify proteins which could bind to TFIIH, HOXC10 was previously reported to be the tightest protein to bind to the CAK complex (58). We therefore explored if HOXC10 binds to endogenous CDK7 in cell lines. HOXC10 weakly co-immunoprecipitated with CDK7 (Figure 6.1). However, upon DNA damage with different chemotherapeutic drugs, the strength of the interaction increased dramatically. Interestingly, the use of different HOXC10-deleted constructs (Figure 6.2) revealed that, contrary to expectation, the homeodomain region of HOXC10 is not necessary to bind to CDK7. Similarly, treating the extracts with ethidium bromide to deplete DNA in the reaction did not affect HOXC10-CDK7 interaction, indicating a DNA-independent protein association between the two (Figure 6.2). These results are unique to HOXC10 as other HOX genes, which despite their non-transcriptional functions, still require the homeodomain region for their interactions (35, 51, 59). Intriguingly, when a predicted high phospho-rich region in HOXC10 was deleted, the binding to CDK7 was significantly reduced.

CDK7 can phosphorylate different sets of proteins depending on whether it is free (i.e. CDK1, 2, 4, 6) or in complex with TFIIH (such as p53, RAR- α , ER, RNA PolIII). We therefore investigated if HOXC10 binding to CDK7 affected its substrate preference. There was no significant difference in CDK1 or CDK2 phosphorylation (at Thr 161 and 160 respectively), ruling out an effect of HOXC10 on free CDK7. Given that RNA PolIII

has a direct role in DNA repair, we next examined if the association of the CAK to the core of the TFIIH complex is modulated by HOXC10. As shown in Figure 6.3, the association of CDK7 with RNA PolII is much stronger in the presence of HOXC10 after DNA damage, allowing transcription to proceed and cells to survive. Further, upon knocking down HOXC10, the kinase activity of CDK7 towards the CTD of RNA Pol II was reduced after DNA damage (with no change in the baseline activity, Figure 6.4).

It has been shown previously that during efficient DNA repair, XPD associates tightly with TFIIH and recruits the CAK complex, which is necessary for resuming transcription of inducible genes, for phosphorylation of proteins involved in the DNA damage response and for preventing improper cell division (42, 60). We therefore examined if HOXC10 affects the composition of the TFIIH-XPD-CAK complex. No direct association between HOXC10 and XPD was detected, nor was a change observed in the binding of XPD to RNA Pol II in the presence or absence of HOXC10. However, as expected, the binding of XPD to CDK7 was reduced upon knockdown of HOXC10, and conversely, was higher following HOXC10 overexpression in the cell lines (Figure 6.5). This suggests that HOXC10 has an essential role in anchoring the CAK to XPD, therefore maintaining the integrity of the holo TFIIH during response to DNA damage. This is also in accordance with previous data showing that in repair-deficient cells, the association of CAK, and not XPD, to the damaged DNA was reduced (61).

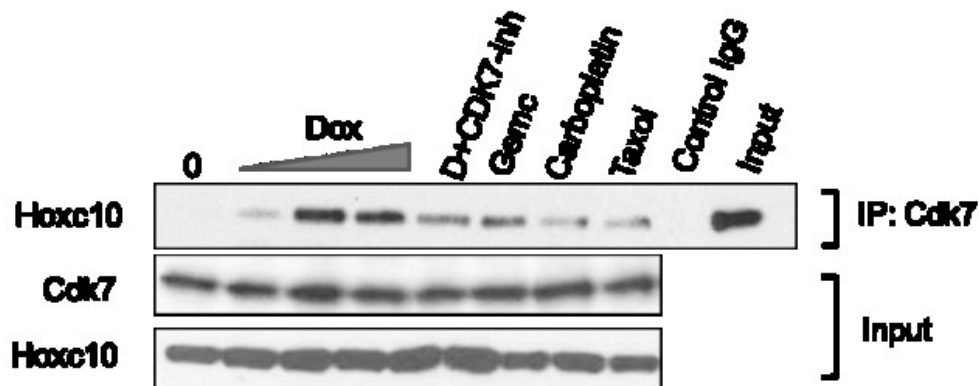


Figure 6.1. HOXC10 binds to CDK7 during DNA damage response. 293T cells were transfected with HOXC10 vector and then treated with different drugs for 24h. Cell lysates were subjected to co-IP with CDK7 (D: Doxorubicin; CDK7-inh: SNS-032).

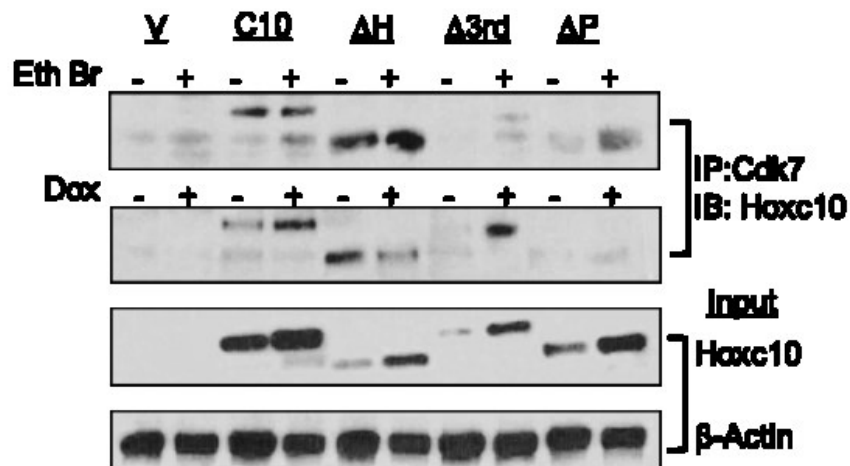


Figure 6.2. HOXC10-CDK7 interaction is independent of HOXC10 DNA binding ability. Different HOXC10 deletion constructs were transfected into 293T, treated with doxorubicin or ethidium bromide (Eth Br) and then co-IP with CDK7 antibodies.

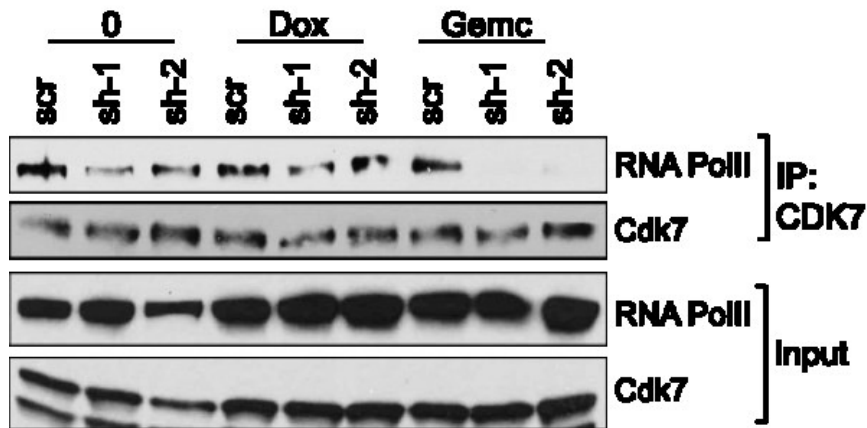
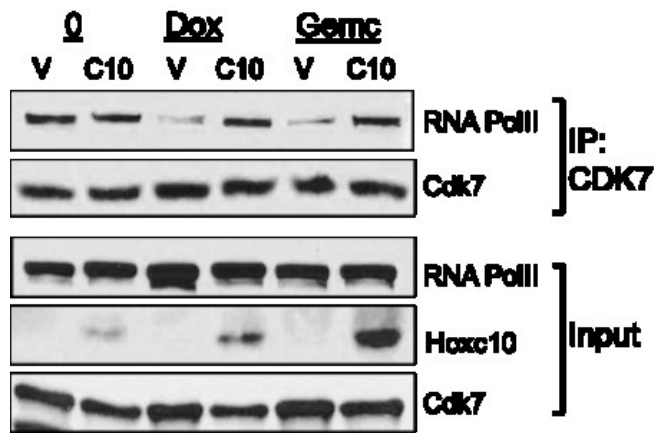


Figure 6.3. CDK7 binds TFIIH more efficiently in the presence of HOXC10. Stable cell lines were treated with dox or gemcitabine for 24h and cell lysates were subjected to IP with CDK7 antibodies. CDK7 association to TFIIH during DNA damage- as detected by RNA Pol II binding- is increased in the presence of HOXC10.

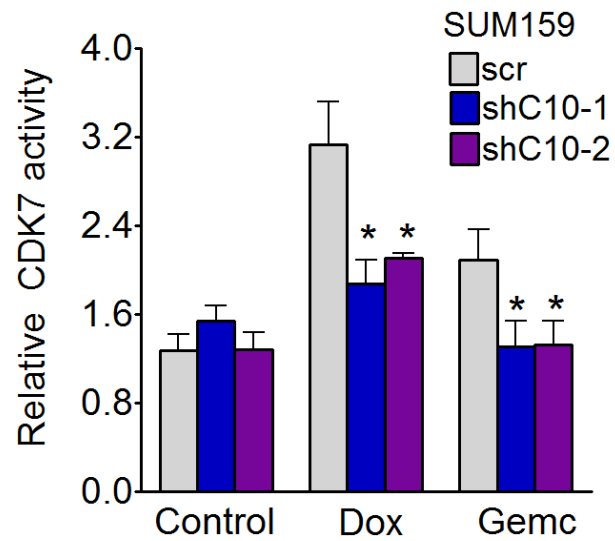


Figure 6.4. CDK7 activity towards RNA Pol II is reduced upon HOXC10 depletion. The kinase activity of CDK7 towards a recombinant GST-CTD substrate was assessed 24h after treatment of SUM159 with 200nM dox or gemcitabine. CTD: C-terminal domain (CTD) of the RNA polymerase II large subunit

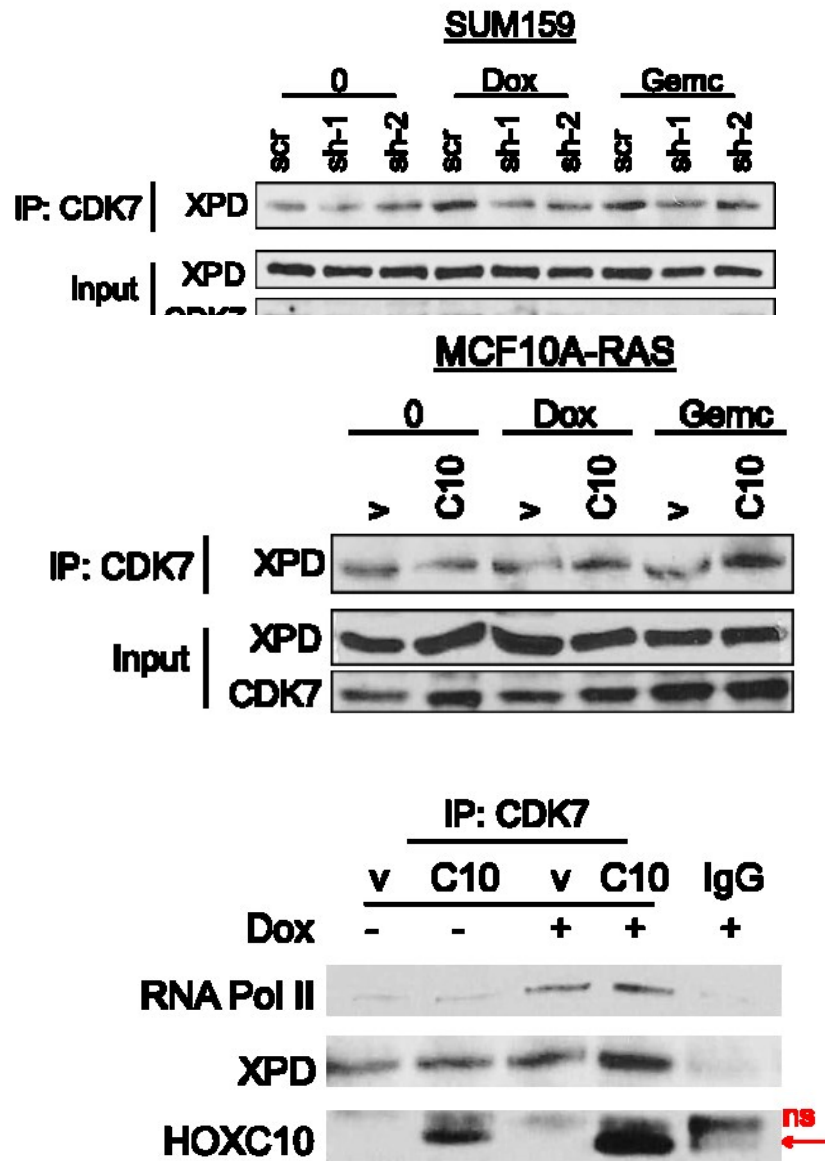


Figure 6.5. CDK7-XPD association is increased upon HOXC10 expression after treatment. XPD was co-immunoprecipitated with CDK7 antibodies in MCF10A-Ras, SUM159 (stable systems) or 293T cells (transiently transfected with vector (v) or HOXC10 expression vectors) after drug treatment for 24h. Indicated proteins were detected by Western blotting.

6.2 Inhibiting CDK7 reverses chemoresistance developed by HOXC10 overexpression

During the last decade, many CDKs were found to be hyperactivated in different cancers, and have become the targets of new therapies, either as single agents or in combination with traditional cytotoxic chemotherapy (62). In particular, inhibiting CDK7 is of special interest as it can affect different signaling pathways, including proliferation, transcription, apoptosis and even ligand-dependent phosphorylation of ER- α in breast cancer (63).

Since HOXC10 drives chemoresistance in part by activating CDK7, and since inhibiting CDK7 is of clinical importance, we next investigated if targeting CDK7 activity in breast cancer can reverse HOXC10's protective effect on survival and therefore restore susceptibility to chemotherapy. First, using siRNA, we reduced CDK7 protein levels by 60%-80%, and then treated cells with different drugs (Figure 6.6, 6.7). Decreasing CDK7 levels in cells slowed down their growth and restored their response to drug treatment, suggesting that the protective effect of HOXC10 during response to chemotherapy was partially abrogated.

Many CDK7 inhibitors have been recently developed, including the selective inhibitor BS-181 (64) and SNS-032 (65) - a drug being evaluated in Phase 1 studies for the treatment of some advanced B-lymphoid or solid malignancies (<http://clinicaltrials.gov/>). We therefore studied the effect of co-treatment with chemotherapy and these 2 CDK7 inhibitors. We used the inhibitors at a concentration that has minimal cytotoxic effect (~20%) as single agent. Adding CDK7 inhibitors to different chemotherapy drugs led to a better response in all cells studied (Figure 6.8). Interestingly, the level of response of SUM159-scr and MCF10A-Ras-C10 with the co-treatment was equal to that of SUM19-

shC10 and MCF10A-Ras-v (respectively) when treated with chemotherapy alone. This result confirms that the activation of CDK7 is the major mechanism through which HOXC10 drives survival after chemotherapy treatment; and therefore, inhibiting CDK7 would be a viable strategy to restore chemo-susceptibility.

To confirm this, we treated Taxol-R and Epirubicin-R MCF7 sublines with BS-181 along with cytotoxic drugs. As shown by MTT and colony survival assays, this co-treatment restored chemo-susceptibility of the cells (Figure 6.9).

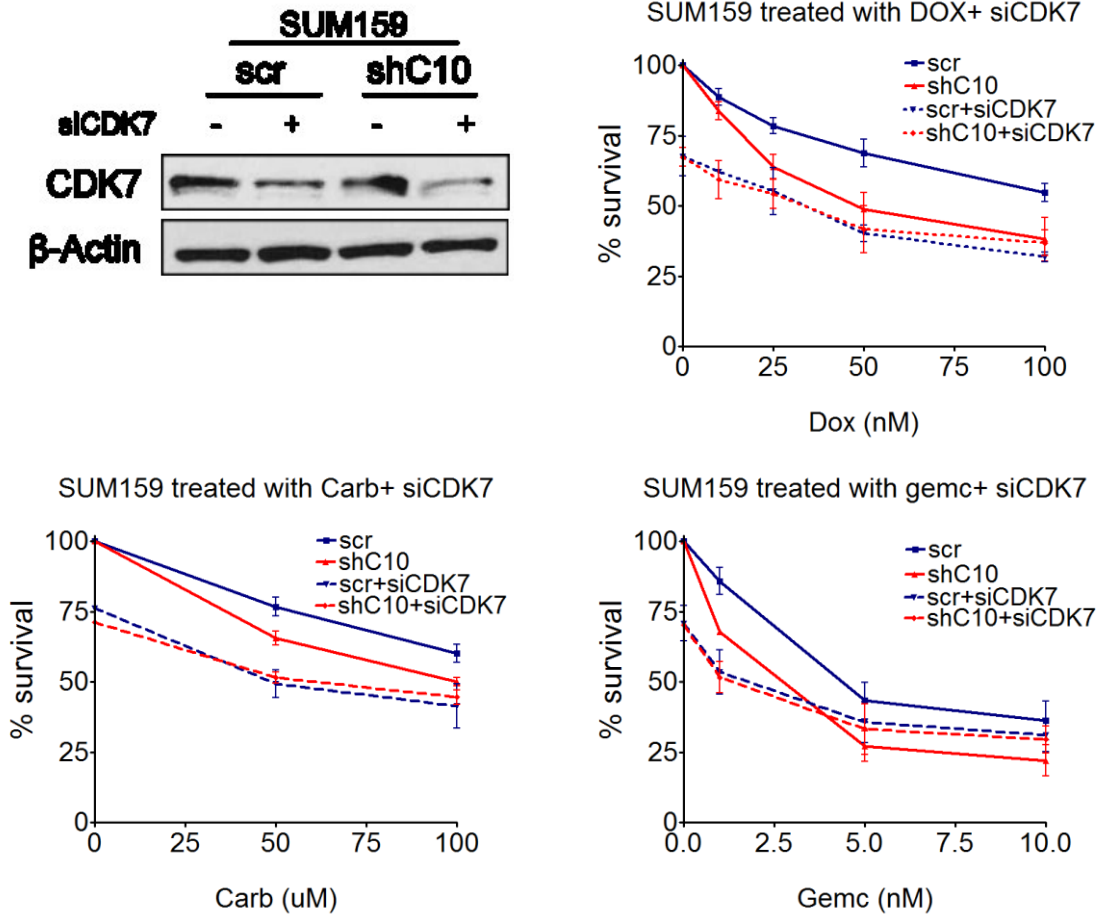


Figure 6.6. CDK7 depletion (approx. 60%) partially restored response to chemotherapy in SUM159. CDK7 was inhibited with siRNA in SUM159 cells. 24h later, cells were treated with doxorubicin, gemcitabine or carboplatin. MTT assay was performed after 48h. The western blot shows a decrease of at least 60% in the protein levels of CDK7 with the siRNA transfection.

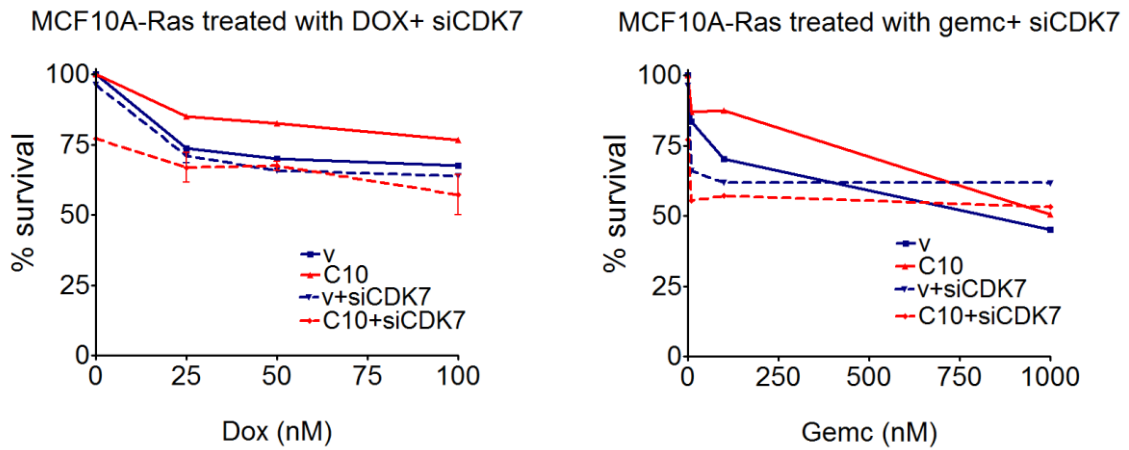
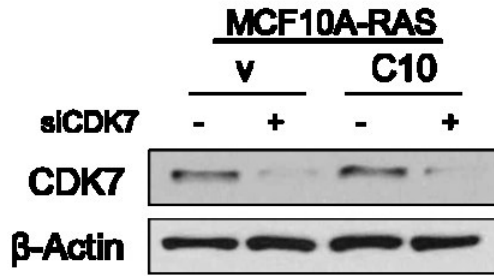
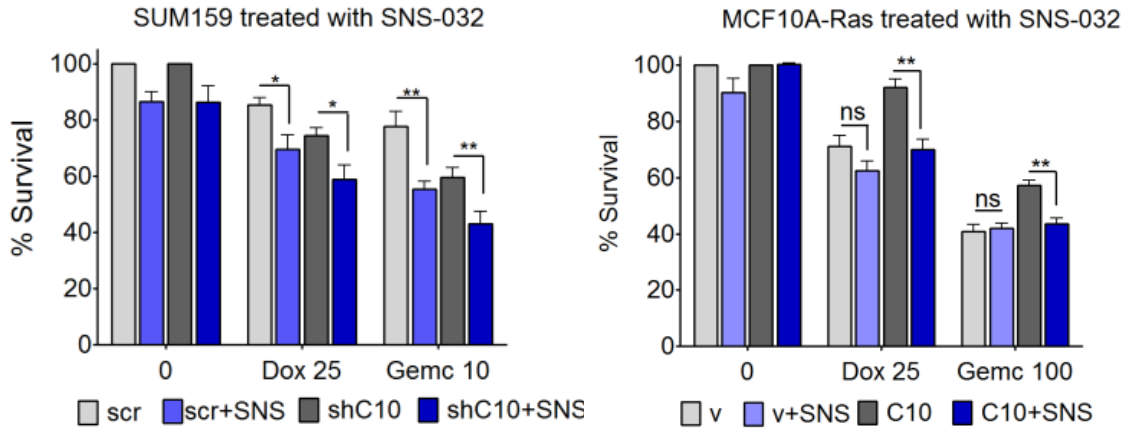


Figure 6.7. CDK7 KD partially restored response to chemotherapy in MCF10A-Ras. CDK7 was inhibited with siRNA in MCF10A-Ras cells. 24h later, cells were treated with doxorubicin or gemcitabine. MTT assay was performed after 48h. The western blot shows a decrease of at least 80% in the protein levels of CDK7 with the siRNA transfection.

A.



B.

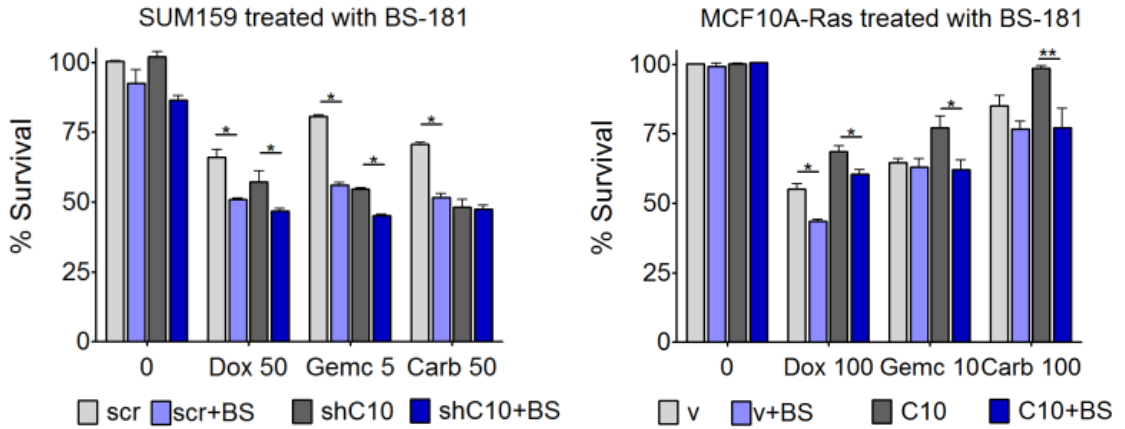
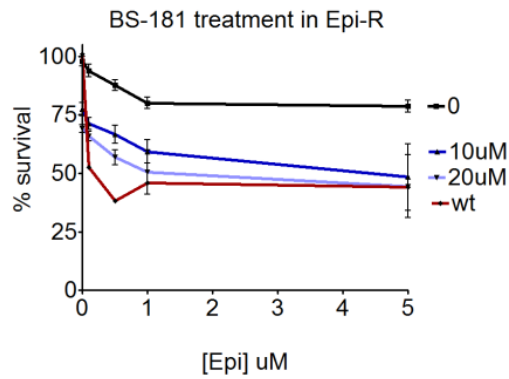
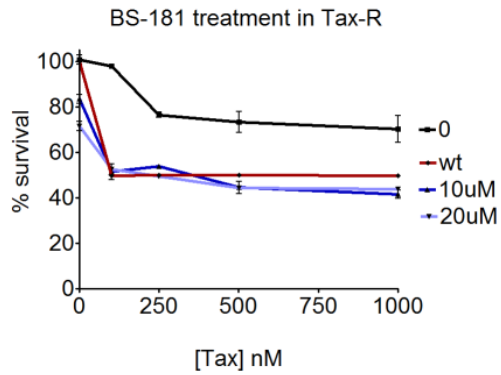


Figure 6.8. CDK7 inhibition by drugs partially restored response to chemotherapy. Cells were co-treated with chemotherapy and with 2 different CDK7 inhibitors, SNS-032 (A) or BS-181 (B). MTT assay was performed after 48h.

A.



B.

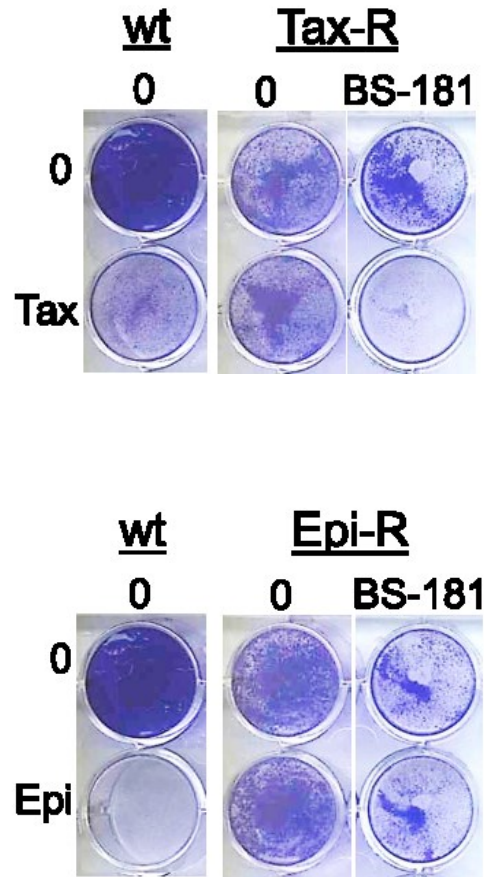


Figure 6.9. CDK7 specific inhibition reduced acquired chemoresistance. A. Taxol or Epirubicin resistant MCF7 cells were treated with taxol or epirubicin respectively in combination with different doses of BS-181. MTT was conducted 48h later. B. Taxol or Epirubicin-resistant MCF7 cells were treated with 200 nM taxol or 500 uM epirubicin alone or in combination with 20uM BS-181. Cells were allowed to grow for 7 days, then surviving colonies were stained with crystal violet.

CHAPTER 7

Discussion

Molecular characteristics of the tumor, pharmaceutical properties of the chemotherapy agents, and the interaction between the cancer, the cancer environment and the drugs are some of the factors that determine the success of the treatment. To overcome the cytotoxic effect of chemotherapy, cancer cells have to continuously re-adapt, by strengthening existing pathways or developing new survival mechanisms. As a result, chemoresistance is almost always a multifactorial process, involving intrinsic and acquired adaptations within the heterogeneous tumor (4, 6). Therefore, in order of targeted or cytotoxic drugs to reach their full therapeutic potential, it is fundamental to have a thorough molecular understanding of resistance mechanisms, to develop solutions to overcome them and to discover reliable predictive and prognostic biomarkers.

In this dissertation, we present evidence for the first time that the overexpression of HOXC10 in breast cancer is not only common and functional, but also prognostic for outcome following chemotherapy treatment. We have shown the following: 1) Chemotherapy resistant cancer cells (selected by continuous in-vivo or in-vitro drug treatment) have upregulated HOXC10 expression; 2) High HOXC10 is functional and important in cancer adaptation mechanisms since exogenously expressing a single gene, HOXC10, led to decrease in drug susceptibility; while decreasing HOXC10 levels by shRNA enhanced cytotoxic effects of chemotherapy. 3) Clinically, in patients treated with chemotherapy, there was a significant correlation between HOXC10 levels and both- poor relapse free survival and poor overall survival.

Mechanistically, HOXC10 is involved in activating different survival pathways. First, HOXC10 is important in driving checkpoint recovery after DNA damage, a key pathway that allow cancer cells to escape the damage response arrest and to continue proliferation after DNA damage. In fact, many factors in this pathway- such as Plk1, Aurora A and Wip1- were found to be upregulated in many cancers and to correlate with aggressiveness, tumor recurrence and poor prognosis (66). We have shown that HOXC10 did not affect the immediate DNA damage response (since there was no difference in the activation of ATM/ATR pathway or in the kinetics of pH2Ax induction). On the other hand, HOXC10 activates DNA repair- mainly the NER pathway- and is required at later stages of DNA damage response (beyond 24h) to allow survival and recovery. Thus, arrested cells which express high levels of HOXC10 have repaired their DNA damage more efficiently and resumed transcription and growth; while their low-HOXC10 expressing counterparts eventually commit to apoptosis. We further show that this can be partially explained by the association of HOXC10 to the CAK subcomplex of the holo TFIIH complex.

The Cdk-activating kinase CAK is composed of the 3 subunits (Cdk7, cyclin H and MAT1), and along with TFIIH, can participate in diverse functions, including transcription, DNA repair (NER) and cell cycle regulation. CDK7 can phosphorylate different substrates: If free, it has preference for CDKs as substrate. Once it is bound to TFIIH, its substrate preference is switched to the C-terminal domain (CTD) of the RNA polymerase II large subunit (67, 68). Previously, in a yeast four-hybrid system, HOXC10 was reported as one among the proteins that bridge the CAK complex to the core TFIIH (58). Here, we have confirmed this interaction and then studied its functional consequence. Interestingly, we found that the homeodomain of HOXC10 is not required for binding to CDK7. To our knowledge, this is the first time that a function of a HOX gene independent

of its homeobox region has been identified. Even though other HOX proteins have been reported to function beyond being transcription factors (by binding to proteins in NHEJ DNA repair pathway (51) or in the DNA replication complex (35, 69), these interactions occurred mainly through the homeodomain motif. The second interesting and unique finding is the presence of a region 5' of the homeodomain that is rich in potential phosphorylation sites and that is important for binding to CDK7. At least 3 of these sites have been reported by phosphoproteomics studies to be actually phosphorylated (www.phosphosite.org, (70)): S189 (during mitosis) and S204 and S206 (in response to UV treatment in HeLa cells; ATM/ATR potential substrates). Other sites have high stringency for CDK5 or CDK1 (T201, T208, S210, S226), or to DNA-PK (S210, S245) (<http://scansite.mit.edu/>, (71)). Though the thorough investigation of the significance of these phosphorylation sites is beyond the scope of this study, we hope this report engenders new interest in studying HOX phosphorylation and their consequence beyond their function as transcription factors.

Functionally, HOXC10 binding to CDK7 increases its kinase activity towards the CTD domain of RNAPII after DNA damage, as revealed by an increase binding of CDK7 to RNAPII, increase CTD phosphorylation and no change in the CDK7-specific phosphorylation sites on CDK1 and CDK2. Previously, it was shown that CAK dissociates from TFIIH within 15 min of UV treatment, and that its kinase activity is neither required for the assembly of the NER machinery nor for repair of photolesions; Instead, its reassociation with the TFIIH within 4h to phosphorylate RNAPII and reinitiate transcription of some genes is essential for the survival and recovery of cells (61, 72, 73). In fact, the failure of the CAK complex to bind to the core TFIIH after DNA damage is a key aberration in the development of the genetic disorder Xeroderma pigmentosum (XP) and of many cancers. We argue here that after DNA damage, HOXC10 plays a key

role in bridging the gap between these 2 complexes, enhancing the recovery process. Indeed, treatment of cells with SNS-032 and BS-181 (inhibitors of CDK7) or with siRNA specifically targeting CDK7, could partially reverse the decrease in susceptibility to chemotherapy treatment upon HOXC10 overexpression.

The importance of our finding to breast cancer therapy stems from the fact that in tumor cells, many of the cell cycle modulators are either upregulated or hyperactivated, leading to uncontrolled cell growth, suggesting that these molecules are promising therapeutic targets. Pan-specific CDK inhibitors are already in clinical development, including flavonoids (alvocidib and P276-00) and purine-based compounds (SNS-032 and seliciclib) but have had limited clinical response as single agents. However, when combined with chemotherapy or targeted therapies, synergistic interactions between the effects of the drugs have been observed, both in vitro and in clinic, making it an attractive approach to overcome resistance (62, 63, 74).

In particular, CDK7 arose as a promising therapeutic target, since it regulates the activities of all other CDKs, thus eliminating the functional compensation seen in targeting individual CDK. It also controls transcription (especially the short half-life transcripts, such as BCL2, Cyclin D, XIAP and MCL1) and the activity of many proteins (such as p53, ER α , RAR α) (62, 68). Due to the synergistic interactions between the effects of CDK7 inhibitors and other chemotherapy drugs, targeting CDK7 became an attractive approach to overcome resistance (63, 75).

The second survival pathway that is activated by HOXC10 is through tipping the balance between growth and apoptosis allowing continuous proliferation and survival under many conditions. We have shown here that HOXC10 facilitates the transition from G1 to S phase and then the progression through the S phase during the cell cycle. As a

consequence, cells with high HOXC10 levels had a growth advantage especially under non-ideal conditions, and were able to restart their replication and transcription to overcome the stressful and toxic conditions. At the same time, the increase in NF- κ B activity and the consequent increase in the levels of many anti-apoptotic proteins decrease the sensitivity of cells to many stressors.

How HOXC10 affects proliferation is still not completely understood. A previous publication hinted a role for HOXC10 in mitotic progression through competing with Cyclin A for binding and degradation by APC in HeLa cells (33). In our breast cancer cells, we could not repeat this finding, nor a correlation between HOXC10 levels and Cyclin A1 protein levels or progression of the cells through G2/M was found. However, we observed that HOXC10 has a function at earlier phases of the cell cycle. This discrepancy is not uncommon, as many cell cycle modulators are known to regulate different checkpoints depending on the cell context (76-78). Recently, many HOX genes- including HOXC10- have been shown to be involved in DNA replication by binding through their homeodomain to the replication machinery complex (Reviewed in (69)). However, none of these studies have investigated the consequence of this binding on cancer progression or survival.

Given the importance of the E2F pathway in G1/S progression and in breast cancer proliferation and prognosis (18), we investigated whether HOXC10 activates this pathway. Interestingly, we found that although E2F1 activity is higher when HOXC10 is overexpressed, some data suggests that this activation is indirect: First, no physical interaction between these two proteins was detected. Second, knockdown of expression of both genes exerted additive- not synergistic- effects on inhibiting proliferation. However, the functional redundancy in the E2F family members precluded detailed investigation, thereby limiting this conclusion. It will be interesting to determine if other

members of the E2F family interact directly with HOXC10. Also, the fact that the DNA binding ability of HOXC10 is necessary to observe increased proliferation suggests that HOXC10 might be binding in the promoter/enhancer region of these genes. A future step is therefore to investigate by ChIP-on-chip the overlaps in HOXC10 and E2F1 binding signatures.

In sum, our model is the following (Figure 7): Under unstressed conditions (A), the major HOXC10 function is in breast cancer cell proliferation- by facilitating the progression of the cells in G1 and S phase. This is achieved through the upregulation of the expression of many proliferation promoting genes, the enhancement of E2F1 activity and the binding to the replication complex. HOXC10 can be bound to the CDK7, bridging the CAK complex to core TFIIH. However, this function is mainly accomplished by XPD. When the cells are exposed to cytotoxic treatment (B), cells arrest at G1 or G2, the CAK complex initially dissociates from RNA Pol II, and the NER factors or other DNA damage response proteins are recruited to recognize and initiate repair. In this situation, HOXC10 switches to a survival factor function: As DNA damage accumulates, it is upregulated, potentially phosphorylated, and more efficiently associated with CDK7 to redirect its kinase activity towards the CTD of RNAPII (C). The result is a better checkpoint recovery, an enhancement of DNA crosslink repair and a decrease in apoptosis, leading to chemotherapy and UV resistance.

Because of its involvement in many survival and proliferation pathways, HOXC10 is an attractive target for breast cancer therapy, especially to reverse resistance. Future studies should be aimed at developing direct inhibitors of HOXC10 (such as microRNAs), or indirect modulators of its function (by targeting its downstream effectors, such as CDK7).

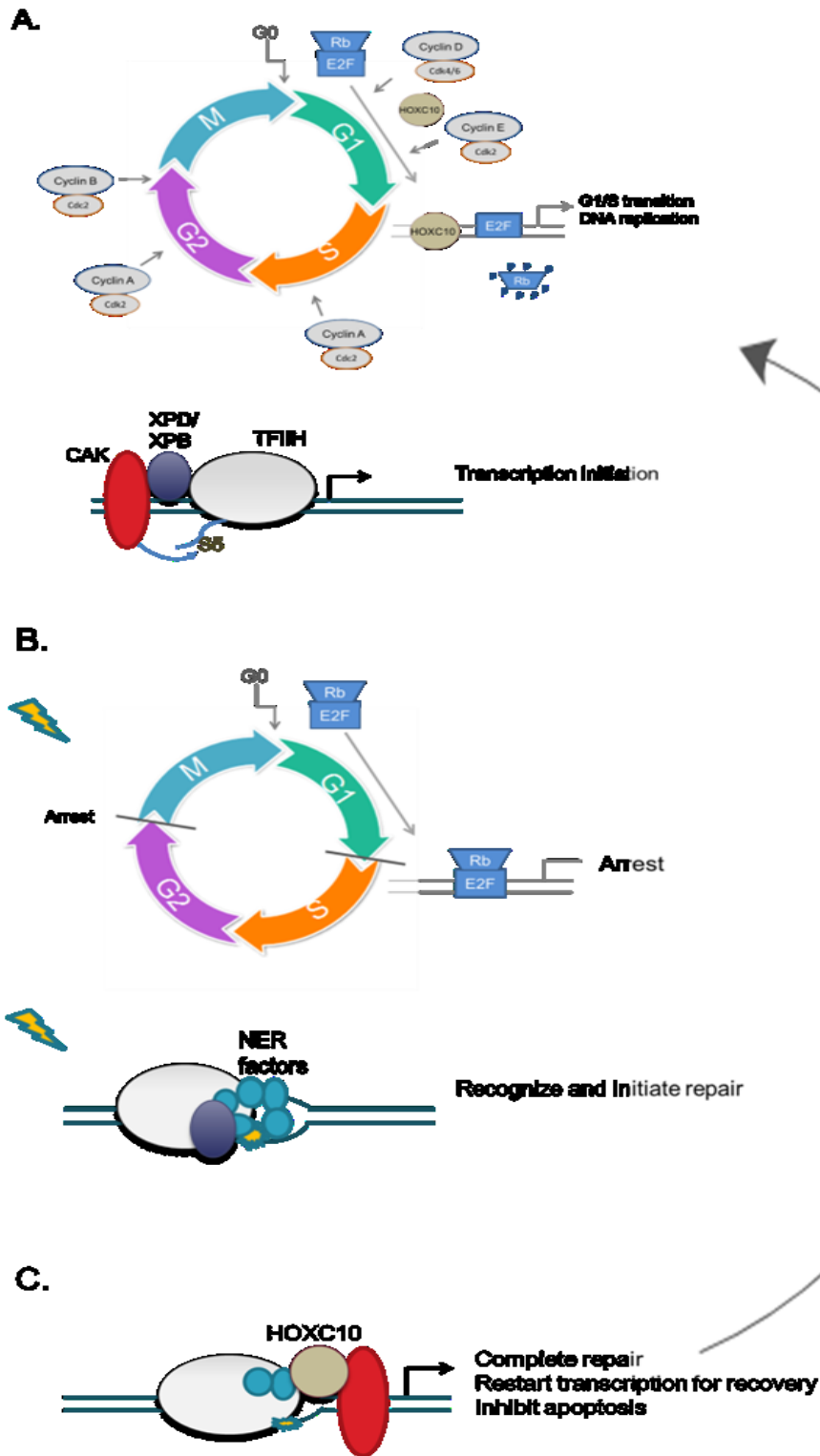


Figure 7. Model of HOXC10 function.

CHAPTER 8

References.

1. DeSantis C, et al., *Breast cancer statistics, 2011*. CA Cancer J Clin, 2011. **61**(6): p. 409-18.
2. Guiu S, et al., *Molecular subclasses of breast cancer: how do we define them? The IMPAKT 2012 Working Group Statement*. Ann Oncol, 2012. **23**(12): p. 2997-3006.
3. Patani N, LA Martin, and M Dowsett, *Biomarkers for the clinical management of breast cancer: international perspective*. Int J Cancer, 2013. **133**(1): p. 1-13.
4. Gonzalez-Angulo AM, F Morales-Vasquez, and GN Hortobagyi, *Overview of resistance to systemic therapy in patients with breast cancer*. Adv Exp Med Biol, 2007. **608**: p. 1-22.
5. Longley DB and PG Johnston, *Molecular mechanisms of drug resistance*. J Pathol, 2005. **205**(2): p. 275-92.
6. Fodale V, et al., *Mechanism of cell adaptation: when and how do cancer cells develop chemoresistance?* Cancer J, 2011. **17**(2): p. 89-95.
7. Mefford D and JA Mefford, *Enumerating the gene sets in breast cancer, a "direct" alternative to hierarchical clustering*. BMC Genomics, 2010. **11**: p. 482.
8. Dai H, et al., *A cell proliferation signature is a marker of extremely poor outcome in a subpopulation of breast cancer patients*. Cancer Res, 2005. **65**(10): p. 4059-66.
9. Desmedt C and C Sotiriou, *Proliferation: the most prominent predictor of clinical outcome in breast cancer*. Cell Cycle, 2006. **5**(19): p. 2198-202.

10. Sotiriou C, et al., *Gene expression profiling in breast cancer: understanding the molecular basis of histologic grade to improve prognosis*. J Natl Cancer Inst, 2006. **98**(4): p. 262-72.
11. Wirapati P, et al., *Meta-analysis of gene expression profiles in breast cancer: toward a unified understanding of breast cancer subtyping and prognosis signatures*. Breast Cancer Res, 2008. **10**(4): p. R65.
12. Whitfield ML, et al., *Common markers of proliferation*. Nat Rev Cancer, 2006. **6**(2): p. 99-106.
13. Han S, et al., *E2F1 expression is related with the poor survival of lymph node-positive breast cancer patients treated with fluorouracil, doxorubicin and cyclophosphamide*. Breast Cancer Res Treat, 2003. **82**(1): p. 11-6.
14. Gorgoulis VG, et al., *Transcription factor E2F-1 acts as a growth-promoting factor and is associated with adverse prognosis in non-small cell lung carcinomas*. J Pathol, 2002. **198**(2): p. 142-56.
15. Salon C, et al., *E2F-1, Skp2 and cyclin E oncoproteins are upregulated and directly correlated in high-grade neuroendocrine lung tumors*. Oncogene, 2007. **26**(48): p. 6927-36.
16. Alla V, et al., *E2F1 in melanoma progression and metastasis*. J Natl Cancer Inst, 2010. **102**(2): p. 127-33.
17. Alla V, et al., *E2F1 confers anticancer drug resistance by targeting ABC transporter family members and Bcl-2 via the p73/DNp73-miR-205 circuitry*. Cell Cycle, 2012. **11**(16): p. 3067-78.
18. Vera J, et al., *Kinetic Modeling-Based Detection of Genetic Signatures That Provide Chemoresistance via the E2F1-p73/DNp73-miR-205 Network*. Cancer Res, 2013. **73**(12): p. 3511-3524.

19. Pallis AG and MV Karamouzis, *DNA repair pathways and their implication in cancer treatment*. *Cancer Metastasis Rev*, 2010. **29**(4): p. 677-85.
20. Selvakumaran M, et al., *Enhanced cisplatin cytotoxicity by disturbing the nucleotide excision repair pathway in ovarian cancer cell lines*. *Cancer Res*, 2003. **63**(6): p. 1311-6.
21. Dabholkar M, et al., *Messenger RNA levels of XPAC and ERCC1 in ovarian cancer tissue correlate with response to platinum-based chemotherapy*. *J Clin Invest*, 1994. **94**(2): p. 703-8.
22. Metzger R, et al., *ERCC1 mRNA levels complement thymidylate synthase mRNA levels in predicting response and survival for gastric cancer patients receiving combination cisplatin and fluorouracil chemotherapy*. *J Clin Oncol*, 1998. **16**(1): p. 309-16.
23. Lord RV, et al., *Low ERCC1 expression correlates with prolonged survival after cisplatin plus gemcitabine chemotherapy in non-small cell lung cancer*. *Clin Cancer Res*, 2002. **8**(7): p. 2286-91.
24. Shirota Y, et al., *ERCC1 and thymidylate synthase mRNA levels predict survival for colorectal cancer patients receiving combination oxaliplatin and fluorouracil chemotherapy*. *J Clin Oncol*, 2001. **19**(23): p. 4298-304.
25. Compe E and JM Egly, *TFIIH: when transcription met DNA repair*. *Nat Rev Mol Cell Biol*, 2012. **13**(6): p. 343-54.
26. Shah N and S Sukumar, *The Hox genes and their roles in oncogenesis*. *Nat Rev Cancer*, 2010. **10**(5): p. 361-71.
27. Jin K, et al., *The HOXB7 protein renders breast cancer cells resistant to tamoxifen through activation of the EGFR pathway*. *Proc Natl Acad Sci U S A*, 2012. **109**(8): p. 2736-41.

28. Shah N, et al., *HOXB13 mediates tamoxifen resistance and invasiveness in human breast cancer by suppressing ERalpha and inducing IL-6 expression*. Cancer Res, 2013.
29. Chen H, S Chung, and S Sukumar, *HOXA5-induced apoptosis in breast cancer cells is mediated by caspases 2 and 8*. Mol Cell Biol, 2004. **24**(2): p. 924-35.
30. Raman V, et al., *Compromised HOXA5 function can limit p53 expression in human breast tumours*. Nature, 2000. **405**(6789): p. 974-8.
31. Chu MC, FB Selam, and HS Taylor, *HOXA10 regulates p53 expression and matrigel invasion in human breast cancer cells*. Cancer Biol Ther, 2004. **3**(6): p. 568-72.
32. Kachgal S, KA Mace, and NJ Boudreau, *The dual roles of homeobox genes in vascularization and wound healing*. Cell Adh Migr, 2012. **6**(6): p. 457-70.
33. Gabellini D, et al., *Early mitotic degradation of the homeoprotein HOXC10 is potentially linked to cell cycle progression*. EMBO J, 2003. **22**(14): p. 3715-24.
34. de Stanchina E, et al., *Selection of homeotic proteins for binding to a human DNA replication origin*. J Mol Biol, 2000. **299**(3): p. 667-80.
35. Marchetti L, et al., *Homeotic proteins participate in the function of human-DNA replication origins*. Nucleic Acids Res, 2010. **38**(22): p. 8105-19.
36. Christen B, et al., *Regeneration-specific expression pattern of three posterior Hox genes*. Dev Dyn, 2003. **226**(2): p. 349-55.
37. Zhai Y, et al., *Gene expression analysis of preinvasive and invasive cervical squamous cell carcinomas identifies HOXC10 as a key mediator of invasion*. Cancer Res, 2007. **67**(21): p. 10163-72.
38. Abba MC, et al., *Breast cancer molecular signatures as determined by SAGE: correlation with lymph node status*. Mol Cancer Res, 2007. **5**(9): p. 881-90.

39. Ansari KI, et al., *HOXC10 is overexpressed in breast cancer and transcriptionally regulated by estrogen via involvement of histone methylases MLL3 and MLL4*. J Mol Endocrinol, 2012. **48**(1): p. 61-75.
40. Gupta RA, et al., *Long non-coding RNA HOTAIR reprograms chromatin state to promote cancer metastasis*. Nature, 2010. **464**(7291): p. 1071-6.
41. Hembruff SL, et al., *Role of drug transporters and drug accumulation in the temporal acquisition of drug resistance*. BMC Cancer, 2008. **8**: p. 318.
42. Chen J, et al., *Xpd/Ercc2 regulates CAK activity and mitotic progression*. Nature, 2003. **424**(6945): p. 228-32.
43. Campanero MR, MI Armstrong, and EK Flemington, *CpG methylation as a mechanism for the regulation of E2F activity*. Proc Natl Acad Sci U S A, 2000. **97**(12): p. 6481-6.
44. Sellers WR, JW Rodgers, and WG Kaelin, Jr., *A potent transrepression domain in the retinoblastoma protein induces a cell cycle arrest when bound to E2F sites*. Proc Natl Acad Sci U S A, 1995. **92**(25): p. 11544-8.
45. Pomerantz JL, EM Denny, and D Baltimore, *CARD11 mediates factor-specific activation of NF-kappaB by the T cell receptor complex*. EMBO J, 2002. **21**(19): p. 5184-94.
46. Veeman MT, et al., *Zebrafish prickle, a modulator of noncanonical Wnt/Fz signaling, regulates gastrulation movements*. Curr Biol, 2003. **13**(8): p. 680-5.
47. Gyorffy B, et al., *An online survival analysis tool to rapidly assess the effect of 22,277 genes on breast cancer prognosis using microarray data of 1,809 patients*. Breast Cancer Res Treat, 2010. **123**(3): p. 725-31.
48. Shaoqiang C, et al., *Expression of HOXD3 correlates with shorter survival in patients with invasive breast cancer*. Clin Exp Metastasis, 2013. **30**(2): p. 155-63.

49. Sun M, et al., *HMGA2/TET1/HOXA9 signaling pathway regulates breast cancer growth and metastasis*. Proc Natl Acad Sci U S A, 2013. **110**(24): p. 9920-5.
50. Gangadharan C, M Thoh, and SK Manna, *Inhibition of constitutive activity of nuclear transcription factor kappaB sensitizes doxorubicin-resistant cells to apoptosis*. J Cell Biochem, 2009. **107**(2): p. 203-13.
51. Rubin E, et al., *A role for the HOXB7 homeodomain protein in DNA repair*. Cancer Res, 2007. **67**(4): p. 1527-35.
52. Johnson JM and JJ Latimer, *Analysis of DNA repair using transfection-based host cell reactivation*. Methods Mol Biol, 2005. **291**: p. 321-35.
53. Pfuhrer S and HU Wolf, *Detection of DNA-crosslinking agents with the alkaline comet assay*. Environ Mol Mutagen, 1996. **27**(3): p. 196-201.
54. Mah LJ, A El-Osta, and TC Karagiannis, *gammaH2AX: a sensitive molecular marker of DNA damage and repair*. Leukemia, 2010. **24**(4): p. 679-86.
55. Huang X, et al., *Assessment of histone H2AX phosphorylation induced by DNA topoisomerase I and II inhibitors topotecan and mitoxantrone and by the DNA cross-linking agent cisplatin*. Cytometry A, 2004. **58**(2): p. 99-110.
56. Olive PL and JP Banath, *Kinetics of H2AX phosphorylation after exposure to cisplatin*. Cytometry B Clin Cytom, 2009. **76**(2): p. 79-90.
57. Banath JP, et al., *Residual gammaH2AX foci as an indication of lethal DNA lesions*. BMC Cancer, 2010. **10**: p. 4.
58. Sandrock B and JM Egly, *A yeast four-hybrid system identifies Cdk-activating kinase as a regulator of the XPD helicase, a subunit of transcription factor IIH*. J Biol Chem, 2001. **276**(38): p. 35328-33.
59. Salsi V, et al., *HOXD13 binds DNA replication origins to promote origin licensing and is inhibited by geminin*. Mol Cell Biol, 2009. **29**(21): p. 5775-88.

60. Cameroni E, K Stettler, and B Suter, *On the traces of XPD: cell cycle matters - untangling the genotype-phenotype relationship of XPD mutations*. Cell Div, 2010. **5**: p. 24.
61. Arab HH, et al., *Dissociation of CAK from core TFIIH reveals a functional link between XP-G/CS and the TFIIH disassembly state*. PLoS One, 2010. **5**(6): p. e11007.
62. Gallorini M, A Cataldi, and V di Giacomo, *Cyclin-dependent kinase modulators and cancer therapy*. BioDrugs, 2012. **26**(6): p. 377-91.
63. Wesierska-Gadek J and MP Kramer, *The impact of multi-targeted cyclin-dependent kinase inhibition in breast cancer cells: clinical implications*. Expert Opin Investig Drugs, 2011. **20**(12): p. 1611-28.
64. Ali S, et al., *The development of a selective cyclin-dependent kinase inhibitor that shows antitumor activity*. Cancer Res, 2009. **69**(15): p. 6208-15.
65. Chen R, et al., *Mechanism of action of SNS-032, a novel cyclin-dependent kinase inhibitor, in chronic lymphocytic leukemia*. Blood, 2009. **113**(19): p. 4637-45.
66. Peng A, *Working hard for recovery: mitotic kinases in the DNA damage checkpoint*. Cell Biosci, 2013. **3**(1): p. 20.
67. Yankulov KY and DL Bentley, *Regulation of CDK7 substrate specificity by MAT1 and TFIIH*. EMBO J, 1997. **16**(7): p. 1638-46.
68. Fisher RP, *Secrets of a double agent: CDK7 in cell-cycle control and transcription*. J Cell Sci, 2005. **118**(Pt 22): p. 5171-80.
69. Miotto B and Y Graba, *Control of DNA replication: a new facet of Hox proteins?* Bioessays, 2010. **32**(9): p. 800-7.
70. Hornbeck PV, et al., *PhosphoSitePlus: a comprehensive resource for investigating the structure and function of experimentally determined post-*

- translational modifications in man and mouse*. Nucleic Acids Res, 2012. **40**(Database issue): p. D261-70.
71. Obenaus JC, LC Cantley, and MB Yaffe, *Scansite 2.0: Proteome-wide prediction of cell signaling interactions using short sequence motifs*. Nucleic Acids Res, 2003. **31**(13): p. 3635-41.
72. Coin F, et al., *Nucleotide excision repair driven by the dissociation of CAK from TFIIH*. Mol Cell, 2008. **31**(1): p. 9-20.
73. Zhu Q, et al., *Lack of CAK complex accumulation at DNA damage sites in XP-B and XP-B/CS fibroblasts reveals differential regulation of CAK anchoring to core TFIIH by XPB and XPD helicases during nucleotide excision repair*. DNA Repair (Amst), 2012. **11**(12): p. 942-50.
74. Malumbres M, et al., *CDK inhibitors in cancer therapy: what is next?* Trends Pharmacol Sci, 2008. **29**(1): p. 16-21.
75. Lolli G and LN Johnson, *CAK-Cyclin-dependent Activating Kinase: a key kinase in cell cycle control and a target for drugs?* Cell Cycle, 2005. **4**(4): p. 572-7.
76. Niculescu AB, 3rd, et al., *Effects of p21(Cip1/Waf1) at both the G1/S and the G2/M cell cycle transitions: pRb is a critical determinant in blocking DNA replication and in preventing endoreduplication*. Mol Cell Biol, 1998. **18**(1): p. 629-43.
77. Zhang C, et al., *Definition of a FoxA1 Cistrome that is crucial for G1 to S-phase cell-cycle transit in castration-resistant prostate cancer*. Cancer Res, 2011. **71**(21): p. 6738-48.
78. Zhu W, PH Giangrande, and JR Nevins, *E2Fs link the control of G1/S and G2/M transcription*. EMBO J, 2004. **23**(23): p. 4615-26.

CURRICULUM VITAE FOR HELEN SADIK

The Johns Hopkins University School of Medicine

Helen Sadik

Created on October 8, 2013

Educational History:

Ph.D. expected	Program in CMM	Johns Hopkins School of Medicine	2013
	Mentor: Saraswati Sukumar, Ph.D.		
B.S	Biology	Lebanese American University	2007

Other Professional Experience

Discovery to Market		JH Carey Business School	2013
FDA's Clinical Investigator Training Course		FDA, Online	2013
Methods for Clinical and Translational Research		JH ICTR	2010

Scholarship and Fellowship

DOD Breast Cancer Research Program grant: Predoctoral fellowship for proposal BC093970 (research support); 2010-2013; \$108,378.00

Scholar-in-Training Award (supported by Aflac Inc.): Travel award to attend the 2nd AACR International Conference in Jordan; March 2010; \$1200

Academic honors

2010	Annual GSA Poster Session (2 nd place)	Johns Hopkins GSA
2007	President award and valedictorian	Lebanese American University
2005	High Distinction Award	Lebanese American University

Publications

Sadik H, Nguyen N, Shah N, Gupta R, Chang HY, and Sukumar S. HOXC10 links proliferation, transcription and DNA repair promoting chemotherapy resistance. **In review.**

Shah N, Jin K, Cruz LA, Park S, **Sadik H**, Cho S, Goswami CP, Nakshatri H, Gupta R, Chang HY, Zhang Z, Cimino-Mathews A, Cope L, Umbricht C, Sukumar S (2013) HOXB13 mediates tamoxifen resistance and invasiveness in human breast cancer by suppressing ER α and inducing IL-6 expression. *Cancer Res.* 73:5449-58.

Gao D, Joshi N, Choi H, Ryu S, Hahn M, Catena R, **Sadik H**, Argani P, Wagner P, Vahdat LT, Port JL, Stiles B, Sukumar S, Altorki NK, Rafii S, Mittal V (2012) Myeloid progenitor cells in the premetastatic lung promote metastases by inducing mesenchymal to epithelial transition. *Cancer Res.* 72:1384–1394.

Lo PK, Lee JS, Liang X, Han L, Mori T, Fackler MJ, **Sadik H**, Argani P, Pandita TK, Sukumar S (2010) Epigenetic inactivation of the potential tumor suppressor gene FOXF1 in breast cancer. *Cancer Res.* 70:6047–6058.

Posters and Abstracts

Sadik H, Nguyen N, Shah N, Gupta R, Chang HY, and Sukumar S. HOXC10, a Homeobox Protein Overexpressed in Breast Cancer, Modulates the Response to Chemotherapy Treatment

(2010, 2012) San Antonio Breast Cancer Symposium, San Antonio, TX; and

(2011) Era of Hope CDMRP conference, Orlando, FL

Sadik H, Shah N, Gupta R, Chang HY, Sukumar S (2010) The Homeobox Protein HOXC10 is Overexpressed in Breast Cancer and Confers Resistance to Doxorubicin. Invited to give a talk at AACR conference (Advances in Cancer Research: From the Laboratory to the Clinic), Dead Sea, Jordan

Service and Leadership

2010-2011 Vice President for Hopkins Dance Club

2009 Tutoring for Principles of Immunology course (CMM program)